# Multiphoton ionization in superintense, high-frequency laser fields. II. Stabilization of atomic hydrogen in linearly polarized fields

Marcel Pont
*Physics Department, University of Southern California, Los Angeles, California 90089-0484*
(Received 2 November 1990; revised manuscript received 27 February 1991)

This is the second of two papers studying multiphoton ionization (MPI) in superintense, high-frequency laser fields. They are based on a general iteration scheme in increasing powers of the inverse frequency. To lowest order in the frequency, i.e., the high-frequency limit, the atom is stable against decay by MPI, though distorted. To next order in the iteration, an expression for the MPI amplitude was obtained. In our first paper [preceding paper, Phys. Rev. A **44**, 2141 (1991)], an alternative expression for the MPI amplitude was obtained for atomic hydrogen, which is substantially simpler, though somewhat less accurate. In the present paper, we study its consequences for the case of atomic hydrogen in superintense, linearly polarized fields with the emphasis on the ground state. Special attention is paid to the case in which the de Broglie wavelength of the photoelectrons is small with respect to the amplitude of oscillation of the (distorted) electronic cloud. This condition defines a radiation regime which yields features in sharp contrast to those obtained in weak fields. Most importantly, the total decay rate decreases with increasing intensity at given (high) frequency ("high-intensity stabilization"). The *angular distributions* of photoelectrons are found to be characterized by rapid oscillations with the polar angle, arising from a peculiar way in which outgoing electron waves interfere. At the same time, the overall behavior of the photoelectrons is to be ejected in directions nearly perpendicular to the polarization axis. We have solved the limit of extremely high intensities at fixed, but otherwise arbitrarily chosen, frequency analytically. We find that in "ultrastrong fields" the *branching ratios* for decay by absorption of the various number of photons possible are only weakly dependent on the values of the intensity and frequency of the laser field, yet excess-photon ionization constitutes a sizable part of the decay modes of the atom (typically 30%). At very high intensities, the hydrogen atom tends to stabilize at fixed, but otherwise arbitrarily chosen frequency. The (*a priori* unexpected) relative stability of the hydrogen atom in ultrastrong fields is explained as a result of "radiative distortion" of the electron cloud and "destructive interference" of outgoing electron waves. Although the lifetime of the atom turns out to be extremely short for values of the intensity around the atomic unit, for low enough frequencies and very high intensities, it can be remarkably long. Finally, we discuss the problem of how the atom subject to these extreme radiation conditions could be observed experimentally.

## I. INTRODUCTION

This is the second of two papers studying multiphoton ionization in superintense, high-frequency laser fields. They are based on a general iteration scheme in increasing powers of the inverse frequency developed by Gavrila and Kaminski [1]. (In this procedure, a certain parameter $\alpha_0$, a combination of the intensity and the frequency, is kept fixed.) The considerations are made in a frame of reference that moves along with a classical electron driven by the laser field, the "Kramers frame of reference." To lowest order in the frequency ("the high-frequency limit"), the atom turns out to be stable against decay by multiphoton ionization. The "radiative distortion" of the electron cloud of the atom and the ac Stark shifts of its levels can be calculated from a Schrödinger equation with a modified atomic binding potential, the "dressed potential," depending on the parameter $\alpha_0$ only. We have studied this in great detail for the case of atomic hydrogen in both linearly [2] and circularly polarized fields [3]. Among other things, we found a drastic decrease of the ionization potential and a dramatic distortion of the electron cloud with increasing $\alpha_0$, resulting in its splitting (for linear polarization) into two separate parts for high values of $\alpha_0$; this feature we called "dichotomy." A brief summary of our findings, together with a recapitulation of the basic equations of the Gavrila-Kaminski scheme (for arbitrary polarization), is given in Secs. I and II of the preceding paper (hereafter referred to as paper I) [4].

To next order in the iteration in increasing powers of the inverse frequency, an expression was obtained for the multiphoton ionization amplitude, in which the bound and continuum solutions of the Schrödinger equation with the dressed potential enter as initial and final states [1] [see Eq. (15) of paper I]. The condition under which the Gavrila-Kaminski theory is applicable requires the photon energy to be large with respect to the ionization potential of the atom in the field, i.e., $\omega \gg |E_0(\alpha_0)|$ [see Eq. (16) of paper I].

In Sec. V of paper I, we derived from the Gavrila-Kaminski result for the multiphoton ionization amplitude a simplified expression applicable to atomic hydrogen in the form of a one-dimensional integral [see Eq. (49) of paper I]

$$f_{\lambda,n} = \frac{1}{\pi k_n^2} \int_{-\pi}^{+\pi} e^{in\phi} e^{i\boldsymbol{\alpha}(\phi)\cdot\mathbf{k}_n} \Phi_\lambda(-\boldsymbol{\alpha}(\phi)) d\phi, \qquad (1)$$

 

from which we can calculate the angular-dependent decay rate for $n$-photon ionization $d\Gamma_{\lambda,n}/d\Omega = k_n|f_{\lambda,n}|^2$ [see Eq. (8) of paper I ].

This could be done for the case of arbitrary polarization. This simplified expression was obtained by neglecting (among others) the attraction of the photoelectron by the dressed potential on its way out (the "final-state interaction"). Here $\Phi_\lambda(\mathbf{r})$ is the spatial part of the (stationary) wave function of a certain (deformed) initial bound state [an eigensolution of the Schrödinger equation with the dressed potential with eigenenergy $E(\alpha_0)$] and pertains to the Kramers reference frame. The vector $\mathbf{k}_n$ is the momentum of the electron ejected from the atom after it has absorbed $n$ photons. Its length is fixed by energy conservation, i.e., $k_n = \sqrt{2[E(\alpha_0) + n\omega]}$ [see Eq. (7) of paper I]. The vector $\boldsymbol{\alpha}(\phi)$ in fact represents the excursion of a free electron driven by the field [and is given by Eqs. (3) and (4) of paper I] with $\phi$ the phase of the laser field. The amplitude of this oscillation is by definition equal to the parameter $\alpha_0$. The above approximation has essentially the same region of validity as the Gavrila-Kaminski expression [5], although it obviously yields less accurate results. It does not, for example, allow for the (weak) asymmetries in the angular distributions of photoelectrons occurring in the case of elliptic polarization that were recently reported by Bashkansky, Bucksbaum, and Shuhmacher [6] as discussed in Sec. III of paper I. As we have pointed out, in the radiation regime where our theory applies, these asymmetries will be weak.

In this paper we will make a detailed study of the angular-dependent and angular-integrated multiphoton ionization decay rates for the case of atomic hydrogen subject to a superintense, high-frequency radiation field of *linear* polarization based on our simplified expression for the multiphoton ionization amplitude, Eq. (1) [7]. In the case of linear polarization, we have $\boldsymbol{\alpha}(\phi) = \alpha_0 \mathbf{e} \cos\phi$, with $\mathbf{e}$ the (real) polarization vector. [See Eq. (3) of our paper I, recalling that for linear polarization $\chi = 0°$.] Thus, in the Kramers reference frame the proton oscillates harmonically along the polarization axis between the turning points $\pm\boldsymbol{\alpha}_0 = \pm\alpha_0\mathbf{e}$. The parameter $\alpha_0$ when expressed in terms of the intensity and frequency is given by $\alpha_0 = I^{1/2}\omega^{-2}$ (in atomic units) [see Eq. (4) of paper I]. (The atomic unit of intensity amounts to $I_0 = 3.51 \times 10^{16}$ W cm$^{-2}$.) Our study will be restricted to $\sigma$ states, which are nonvanishing on the polarization axis.

As we have shown in Sec. V of paper I, this simplified expression can be cast in the equivalent form of an (infinite) sum of Bessel functions. For the case of linear polarization this yields [see Eqs. (53) and (59) of paper I]

$$f_{\lambda,n} = \frac{2}{k_n^2} \sum_{m=-\infty}^{+\infty} i^{n-m} J_{n-m}(\boldsymbol{\alpha}_0 \cdot \mathbf{k}_n) \Phi_{\lambda,m}. \tag{2}$$

The coefficients $\Phi_{\lambda,m}$ appearing in this equation were given in Eq. (52) of paper I by the Fourier coefficients of the periodic $\Phi_\lambda(-\boldsymbol{\alpha}_0 \cos\phi)$:

$$\Phi_\lambda(-\boldsymbol{\alpha}(\phi)) = \sum_{m=-\infty}^{+\infty} e^{im\phi} \Phi_{\lambda,m}. \tag{3}$$

Henceforth we will drop the subscript $\lambda$, which specifies the decaying state of interest. It is convenient to choose the positive $z$ axis of our coordinate system along $\mathbf{e}$.

Equation (2) enables us to analyze and compute important physical quantities which can be inferred from experiment, such as the lifetime of the atom, the angular distributions of the photoelectrons, and the peak pattern in their energy spectrum.

In Sec. II we present our *analytical results*. We develop our analysis only for the case that the de Broglie wavelength of the photoelectrons ($2\pi/k_n$) is small with respect to the amplitude of oscillation of the atomic electron cloud ($\alpha_0$). This condition defines a radiation regime which yields features in sharp contrast to those obtained in weak fields by lowest-order perturbation theory (LOPT). We have called it the *highly nonperturbative radiation regime*. We study successively angular-dependent and angular-integrated multiphoton ionization decay rates. Finally, we analyze the special case of high $\alpha_0$ in which "atomic dichotomy" occurs. This latter radiation regime corresponds to the limit of extremely high intensities at fixed, but otherwise arbitrarily, chosen frequency. We will refer to it as the *ultrastrong-field limit*. There exist several calculations (Keldysh [8], Mittleman [9], Pert [10], Reiss [11]) that purport to give the ionization probability for an asymptotically large intensity by using a procedure in which the electron-field interaction is taken to be large compared with the electron-nucleus interaction. In these calculations, the modification of the final state by the field is incorporated to all orders through the use of a Volkov state [12], in a similar way as in our expression Eq. (43) of paper I. On the other hand, in these approaches the deformation of the initial state was neglected. It was realized by Mittleman that such an approach leads to results that are in serious error at high intensities [13]. A formalism was proposed by Mittleman in which also the distortion of the initial state could be included. This formalism was applied by Janjusevic and Mittleman to the case of atomic hydrogen [14]. However, it has now been realized that the procedure followed in Refs. [13] and [14] is incorrect [15].

Numerical results and discussion of angular-dependent, partial and total decay rates for multiphoton ionization from the ground state of atomic hydrogen in superintense, high-frequency laser fields are discussed in Sec. III. Finally in Sec. IV we discuss the problem of how the atom subject to these extreme radiation conditions could be observed in an experiment.

Before focusing our attention on the highly nonperturbative radiation regime, defined by $\alpha_0 k_n \gg 1$, let us briefly comment here on the relation of Eq. (1) to LOPT. For low enough intensities, $\alpha_0$ is small and we have, from Eq. (3),

$$\Phi_m \simeq \Phi(\mathbf{0})\delta_{m,0}, \tag{4}$$

where $\Phi(\mathbf{0})$ denotes the value of the *unperturbed* initial state (which we assume here to be of $s$ symmetry) at the origin. Moreover, on top of $\alpha_0 \ll 1$ we also have $\alpha_0 k_n \ll 1$ and we may replace the Bessel functions in Eq. (2) by their small argument behavior [16]:

$$J_n(x) \simeq \frac{1}{n!}\left(\frac{x}{2}\right)^n. \tag{5}$$

The application of Eqs. (4) and (5) in Eq. (2) yields (retaining only the lowest-order term in powers of the intensity, which corresponds to single-photon ionization)

$$\frac{d\Gamma}{d\Omega} = \frac{\alpha_0^2}{k}|\mathbf{e}\cdot\mathbf{e}_k|^2|\Phi(\mathbf{0})|^2 \simeq \frac{I}{\sqrt{2}\omega^{9/2}}|\mathbf{e}\cdot\mathbf{e}_k|^2|\Phi(\mathbf{0})|^2, \tag{6}$$

where $\mathbf{e}_k$ denotes the unit vector in the direction of $\mathbf{k}$. In the last step we have set $\alpha_0 = I^{1/2}\omega^{-2}$ and $k \simeq \sqrt{2\omega}$ [we used $k_n = \sqrt{2[E(\alpha_0) + n\omega]}$, for the case of single-photon ionization, and invoked the condition of high-frequency $\omega \gg |E_0(\alpha_0)|$]. For the ground state of atomic hydrogen we have $|\Phi(\mathbf{0})|^2 = 1/\pi$ and we find Eq. (6) is identical to the high-frequency form of the LOPT result, Eq. (41) of paper I. This demonstrates that if $\alpha_0 k_n \ll 1$ and $\alpha_0 \ll 1$, Eq. (2) yields results which are in agreement with LOPT. As we know, the parameter $\alpha_0$ characterizes the degree of "radiative distortion" of the electron cloud (see Ref. [2]). As will become apparent in the following, the parameter $\alpha_0 k_n$ is a measure of "destructive interference" of outgoing electron waves. LOPT applies when the influence of both is negligible; as will become apparent, the reason why in LOPT the decay rate increases with increasing intensity (at fixed frequency) is due to the fact that if $\alpha_0 k_n \ll 1$, we have "constructive interference" of electron waves. Destructive interference leads to high-intensity stabilization (see Sec. II C).

## II. THE HIGHLY NONPERTURBATIVE RADIATION REGIME

Expressions for the angular-dependent and angular-integrated rates at which electrons are ejected from the atom by single- or excess-photon ionization in a superintense, high-frequency laser field simplify if the condition

$$\alpha_0 k_n \gg 1 \tag{7}$$

is satisfied. This leads to results which are in strong contrast to those obtained from LOPT. They characterize what we have called the highly nonperturbative radiation regime. It is important to be aware of the fact that for moderately high frequency, both conditions, the condition of high frequency, i.e., $\omega \gg |E_0(\alpha_0)|$, and (7) above, can be satisfied arbitrarily well if the intensity is taken sufficiently large. This is due to the decrease of the ionization potential of the atom (within a manifold of states with the same magnetic quantum number as the initial state) with increasing $\alpha_0$, which we have discussed earlier (see Ref. [2]).

In the following sections we will focus on the analysis of the physics described by Eq. (2) in the highly nonperturbative radiation regime. In Sec. II A we study angular-dependent decay rates for single- and excess-photon ionization. Section II B is devoted to angle-integrated decay rates. Finally, in Sec. II C we study the special case of ultrastrong fields (high $\alpha_0$) in which atomic dichotomy occurs.

### A. Angular-dependent multiphoton ionization decay rates

If $|\boldsymbol{\alpha}_0\cdot\mathbf{k}_n| \gg 1$ we may replace the Bessel functions in the sum of Eq. (2) by their well-known asymptotic behavior for large arguments [17]:

$$J_m(x) \underset{x\to\infty}{\sim} \left(\frac{2}{\pi x}\right)^{1/2}\cos\left(x - \frac{1}{2}m\pi - \frac{\pi}{4}\right). \tag{8}$$

(We assume for the moment that $\boldsymbol{\alpha}_0\cdot\mathbf{k}_n > 0$.) The substitution of this into Eq. (2) yields

$$f_n = \frac{i^n}{k_n^2}\left(\frac{2}{\pi|\boldsymbol{\alpha}_0\cdot\mathbf{k}_n|}\right)^{1/2} \times[\Phi(-\boldsymbol{\alpha}_0)e^{+i[\boldsymbol{\alpha}_0\cdot\mathbf{k}_n-(1/2)n\pi-\pi/4]} + \Phi(+\boldsymbol{\alpha}_0)e^{-i[\boldsymbol{\alpha}_0\cdot\mathbf{k}_n-(1/2)n\pi-\pi/4]}], \tag{9}$$

where the summation with respect to $m$ in Eq. (2) was carried out with the help of the relation (3). A similar result holds for $\boldsymbol{\alpha}_0\cdot\mathbf{k}_n < 0$. From Eq. (9) we have, for $\sigma_g$ states,

$$\frac{d\Gamma_n}{d\Omega} = \frac{8|\Phi(\boldsymbol{\alpha}_0)|^2}{\pi k_n^3}\frac{\cos^2(|\boldsymbol{\alpha}_0\cdot\mathbf{k}_n| - \frac{1}{2}n\pi - \pi/4)}{|\boldsymbol{\alpha}_0\cdot\mathbf{k}_n|}, \tag{10}$$

valid for $|\boldsymbol{\alpha}_0\cdot\mathbf{k}_n| \gg 1$, i.e., it does not hold for directions that are nearly perpendicular to the polarization axis. For ungerade states the cosine must be replaced by the sine function. Note that the angular dependence is universal in the sense that it does not depend on the *shape* of the (radiatively distorted) initial state.

According to Eq. (10), the rate at which electrons are ejected contains regular oscillations between zero and two times the value

$$\left(\frac{d\Gamma_n}{d\Omega}\right)^{\text{av}} = \frac{4|\Phi(\boldsymbol{\alpha}_0)|^2}{\pi\alpha_0 k_n^4\cos\theta}. \tag{11}$$

This shows that, having averaged out the rapid oscillations in angle, the multiphoton ionization decay rate depends on the polar angle as $1/\cos\theta$, independent of the intensity, the frequency, and the number of photons absorbed. This angular dependence differs drastically from what is found in weak fields. In (relatively) weak fields the electrons are preferentially ejected in the direction of the polarization (see, e.g., Leuchs and Walther in Chap. 5 of [18], Humpert *et al.* [19], and Wolff *et al.* [20]). In the particular case of single-photon ionization we have, according to LOPT, a $\cos^2\theta$ dependence. One would expect from a semiclassical point of view that the distribution of photoelectrons becomes more peaked in the polarization direction as the number of excess photons increases, since the electric field acts in the polarization direction. This is in strong contrast with the present case where the electrons leave the atom preferentially in directions away from the polarization axis.

In LOPT we have the selection rule $\Delta l = \pm 1$ associated with each absorbed photon, so that for $n$-photon ionization from an $s$ state, the final state consists of partial waves up to orbital angular momentum $l = n$. It is apparent from the angular dependence determined by Eq. (10) that in the highly nonperturbative radiation regime many $l$ waves contribute. One would need to go to very high order in perturbation theory to reproduce the angular dependence given by Eq. (10).

Equation (10) has an interesting *physical interpretation*. This becomes more transparent if we write Eq. (9) in the form

$$f_n = f_- + (-1)^n f_+, \tag{12}$$

where

$$f_\pm = \Phi(\pm\boldsymbol{\alpha}_0) e^{\mp i(\boldsymbol{\alpha}_0 \cdot \mathbf{k}_n)} \left(\frac{2}{\pi|\boldsymbol{\alpha}_0 \cdot \mathbf{k}_n|}\right)^{1/2} \times \frac{\exp[\pm i(\pi/4)\mathrm{sgn}(\boldsymbol{\alpha}_0 \cdot \mathbf{k}_n)]}{k_n^2}, \tag{13}$$

valid for $|\boldsymbol{\alpha}_0 \cdot \mathbf{k}_n| \gg 1$.

Equations (12) and (13) suggest that the oscillations in Eq. (10) arise from the interference of electron waves that are emitted from two sources. The proportionality factors $\Phi(\pm\boldsymbol{\alpha}_0)$, on the one hand, and the phase factors $e^{\mp i(\boldsymbol{\alpha}_0 \cdot \mathbf{k}_n)}$, on the other hand, suggest that the source, associated with the amplitude $f_+$, is located at $\mathbf{r} = +\boldsymbol{\alpha}_0$, and the other, associated with the amplitude $f_-$, at $\mathbf{r} = -\boldsymbol{\alpha}_0$. The two sources are the image of one another after a reflection in the $xy$ plane. (Reflection in the $xy$ plane corresponds to replacing $\mathbf{k}_n$ by $-\mathbf{k}_n$, since we have axial symmetry around the axis of polarization.) Furthermore, the factor $(-1)^n$ in Eq. (12) can be seen to be related to the fact that the two sources are out of phase by precisely half the oscillation time of the laser field. (If ungerade states are considered there is an extra phase factor $-1$ involved.) Without the coherence of the two sources, the oscillations in $d\Gamma_n/d\Omega$ would not appear and we would obtain Eq. (11). [In that case, we would have the sum of the squared modulus of each amplitude in Eq. (12) and not the squared modulus of their sum.] In Appendix A the above given interpretation to Eq. (10) is justified by explicit construction of an *effective* density of sources which yields *exactly* the ionization amplitude given by Eqs. (12) and (13).

From the above discussion we obtain the following physical picture in the laboratory frame of reference: The angular pattern of photoelectrons arises from the interference of (freely propagating) outgoing electron waves that are created in the near vicinity of the proton each time that the distorted electron cloud, which oscillates like a free-electron driven by the field, reaches its turning points. From this it is clear that Eq. (7) is a condition for the occurrence of interference oscillations in the angular dependence of photoelectrons; it requires the de Broglie wavelength of the emitted electron waves to be small with respect to the distance between the two sources.

From Eq. (10) we see that maximal constructive interference between waves emitted from the two sources takes place in the direction

$$\cos\theta = \frac{\pi[q + \frac{1}{2}(n+P) + \frac{1}{4}]}{\alpha_0 k_n}, \tag{14}$$

with $q$ an arbitrary integer. Here $P$ denotes the parity quantum number, which equals 0 (1) for gerade (ungerade) states. Maximal destructive interference takes place in the direction

$$\cos\theta = \frac{\pi[q + \frac{1}{2}(n+P) - \frac{1}{4}]}{\alpha_0 k_n}. \tag{15}$$

The width of the interference fringes (the distance between two successive maxima or minima) is therefore

$$\Delta\theta \approx \frac{\pi}{\alpha_0 k_n \sin\theta}. \tag{16}$$

From this it is easily seen that this width decreases gradually if the angle $\theta$ is increased from the polarization axis to directions perpendicular to it. It is easily shown from Eq. (14) or (15) that the number of interference fringes for $\theta$ between 0° and 180° is approximately equal to $2\alpha_0 k_n/\pi$.

It is interesting to express the condition Eq. (7), which characterizes the highly nonperturbative radiation regime, in an alternative form. By invoking $\alpha_0 = I^{1/2}/\omega^2$ and our high-frequency condition, i.e., $\omega \gg |E_0(\alpha_0)|$, Eq. (7) can be expressed as

$$\frac{I}{4\omega^2} \gg \omega, \tag{17}$$

where we have required the validity of Eq. (7) for all open channels. Equation (17) states that *the energy in the jitter motion of a free electron* driven by the laser field has to be large with respect to *the photon energy* [21].

Angular integration of Eq. (10) leads to divergence. There is no internal inconsistency, however, since the divergence comes from the behavior of $d\Gamma_n/d\Omega$ as the polar angle $\theta$ tends to 90°, whereas Eq. (10) does not apply to directions that are (nearly) orthogonal to the polarization axis. The calculation of the partial decay rates $\Gamma_n$—starting from Eq. (1) or Eq. (2) with which it is equivalent and which yields a finite result for $d\Gamma_n/d\Omega$ ($\theta = 90°$) [see Eq. (63) of paper I]—is carried out in Sec. II B.

### B. Angular-integrated multiphoton ionization decay rates

From Eq. (2) we find that the angular-integrated decay rates can be expressed as the double sum

$$\Gamma_n = \left(\frac{2}{k_n}\right)^4 \frac{\pi}{\alpha_0} {\sum_{p,q}}' (-1)^{[(p-q)/2]} \Phi_{n-p} \Phi^*_{n-q} I_{p,q}(\alpha_0 k_n), \tag{18}$$

where the prime indicates that the summation is to be carried out over all $p$ and $q$ for which $p+q$ is even. In Eq.(18) we have defined the integral $I_{p,q}(x)$ by

$$I_{p,q}(x) = \int_0^x J_p(\tau) J_q(\tau) d\tau. \tag{19}$$

This integral cannot be evaluated in closed form; however, it is possible to obtain an asymptotic expression for $x$ sufficiently large (see Appendix B):

$$I_{p,q}(x) = \frac{(-1)^{[(p-q)/2]}}{\pi}\left[\ln(2x) - \psi\left(\frac{p+q+1}{2}\right) - \psi\left(\frac{p-q+1}{2}\right) + \psi\left(\frac{1}{2}\right)\right] + O(x^{-1}), \tag{20}$$

in which $\psi$ denotes, as usual, the logarithmic derivative of the $\Gamma$ function. The substitution of the expression Eq. (20) into the sum of Eq. (18) yields, for $\Gamma_n$,

$$\Gamma_n = \left(\frac{2}{k_n}\right)^4 \frac{1}{\alpha_0}\{ [\ln(2\alpha_0\, k_n) - \psi(\tfrac{1}{2})]S_n^{(1)}(\alpha_0) + S_n^{(2)}(\alpha_0)\}. \quad (21)$$

In this equation the sums $S_n^{(1)}(\alpha_0)$ and $S_n^{(2)}(\alpha_0)$ are given by the expressions

$$S_n^{(1)} = \sum_{p,q}{}' \Phi_{n-p}\Phi^*_{n-q} \quad (22)$$

and

$$S_n^{(2)} = \sum_{p,q}{}' \Phi_{n-p}\Phi^*_{n-q}\left[ 2\psi\left(\frac{1}{2}\right) - \psi\left(\frac{p+q+1}{2}\right) - \psi\left(\frac{p-q+1}{2}\right)\right], \quad (23)$$

respectively. The sum $S_n^{(1)}$ is readily evaluated from the Fourier series Eq.(3), yielding

$$S_n^{(1)} = |\Phi(\boldsymbol{\alpha}_0)|^2 \quad (24)$$

(it is assumed that $\Phi$ has a definite parity). The evaluation of $S_n^{(2)}$ is more cumbersome and is carried out in Appendix C. It equals

$$S_n^{(2)} = 2\int_0^{\pi/2} \frac{|\Phi(\boldsymbol{\alpha}_0\cos\phi)|^2\cos^2 n\phi - |\Phi(\boldsymbol{\alpha}_0)|^2}{\sin\phi} d\phi. \quad (25)$$

With Eqs. (24) and (25), Eq. (21) yields

$$\Gamma_n = \left(\frac{2}{k_n}\right)^4 \frac{|\Phi(\boldsymbol{\alpha}_0)|^2}{\alpha_0}\left[\ln(2\alpha_0 k_n) - \psi(\tfrac{1}{2}) + \Delta_n(\alpha_0)\right], \quad (26)$$

where we have defined $\Delta_n(\alpha_0)$ by

$$\Delta_n = S_n^{(2)}/|\Phi(\boldsymbol{\alpha}_0)|^2, \quad (27)$$

or equivalently by [see Eq. (25)]

$$\Delta_n = 2\int_0^{\pi/2} \frac{|\Phi(\boldsymbol{\alpha}_0\cos\phi)|^2\cos^2 n\phi - |\Phi(\boldsymbol{\alpha}_0)|^2}{|\Phi(\boldsymbol{\alpha}_0)|^2\sin\phi} d\phi. \quad (28)$$

Equation (26) demonstrates explicitly that (partial) decay rates vanish rapidly with increasing frequency at fixed $\alpha_0$, namely roughly as $k_n^{-4} \propto \omega^{-2}$. Note that the vanishing of the partial rates with increasing $\omega$ at fixed $\alpha_0$ is in accordance with the general theory, summarized in Sec. II of paper I (high-frequency stabilization). The dependence of the partial decay rate, Eqs. (26) and (28), on the intensity, the frequency, and the number of photons absorbed is rather intricate, as could be expected from the nonperturbative nature of our theory. As it turns out, in the special case of high $\alpha_0$ (the ultrastrong-field limit) this dependence is greatly simplified. This we will discuss in Sec. II C. For high-lying Rydberg states one may neglect the atomic distortion, i.e., the implicit $\alpha_0$ dependence in Eq. (26). We then find that at fixed frequency the rates decrease as $I^{-1/2}$, hence *high-intensity stabilization.*

### C. Partial and total multiphoton ionization decay rates in ultrastrong fields (high $\alpha_0$)

Equation (26) can be further analyzed under the condition that $\alpha_0$ is large:

$$\alpha_0 \gg 1. \quad (29)$$

If we keep the frequency fixed and let the intensity grow large, it is easily checked that the three following conditions, namely the condition of high frequency: $\omega \gg |E_0(\alpha_0)|$, the condition of destructive interference: $\alpha_0 k_n \gg 1$ [see Eq. (7)], and the condition of dichotomy: $\alpha_0 \gg 1$ [see Eq. (29) above], can be satisfied arbitrarily well *irrespective of the value of the frequency.* This is so because the binding energy of the ground state (within a manifold of states defined by the magnetic quantum number of the initial state) tends to zero as $\alpha_0$ becomes very large. We have termed the radiation regime, which is characterized by these *three simultaneous conditions*, the "ultrastrong-field limit."

We have shown earlier that in fields of high $\alpha_0$ the bound-state eigenfunctions of the dressed potential split into two parts, each of which is concentrated near either of the two end points of the line segment of charge generating the dressed potential, i.e., $\pm\boldsymbol{\alpha}_0$, and is negligible elsewhere. We have called this phenomenon the "dichotomy" of the hydrogen atom (see Ref. [2]).

Let us give here a short summary of our findings. Since each of the two parts of the wave function separately satisfies approximately the Schrödinger equation for the same value of the energy, the eigenfunctions of $V_0$ appear in "gerade-ungerade" pairs:

$$\Phi_P(\mathbf{r}) = \frac{\chi(\mathbf{r}-\boldsymbol{\alpha}_0) + (-1)^P\chi(-\mathbf{r}-\boldsymbol{\alpha}_0)}{\sqrt{2}}, \quad (30)$$

with $P$ the parity 0 or 1. [We will assume here that $\chi(\mathbf{r})$ is normalized to unity.] Near each end point the dressed potential attains a simpler form. It was shown (see Ref. [2]) that the eigenfunctions and eigenvalues of the Schrödinger equation containing the "end-point potential" scale with $\alpha_0$. It was shown that $\chi(\mathbf{r})$ satisfies the scaling law

$$\chi(\mathbf{r}) = \frac{u(\alpha_0^{-1/3}\mathbf{r})}{\sqrt{\alpha_0}}, \quad (31)$$

while the energy $E$ can be expressed as $E = W\,\alpha_0^{-2/3}$. Here $u(\mathbf{r})$ is an eigenfunction of the Schrödinger equation

$$\left[-\frac{1}{2}\nabla^2 - \frac{1}{\pi}\left(\frac{2}{r}\right)^{1/2} K\left[\left(\frac{1-\cos\theta}{2}\right)^{1/2}\right]\right] u(\mathbf{r}) = W\, u(\mathbf{r}), \quad (32)$$

with energy eigenvalue $W$, independent of $\alpha_0$. Here $K$ denotes as usual the complete elliptic integral of the first kind. The potential entering Eq. (32) is in fact the end-point potential for $\alpha_0 = 1$. [We assume that the eigen-

functions $u(\mathbf{r})$ are normalized to unity.]

From Eqs. (30) and (31) we find in particular that, for sufficiently high $\alpha_0$, the probability density to find the electron at the end points $\pm\boldsymbol{\alpha}_0$ of the line charge is given by

$$|\Phi(\pm\boldsymbol{\alpha}_0)|^2 = \frac{|u(0)|^2}{2\alpha_0}, \tag{33}$$

where the overlap between the functions $\chi(-\mathbf{r}-\boldsymbol{\alpha}_0)$ and $\chi(\mathbf{r}-\boldsymbol{\alpha}_0)$ was neglected. From Eq. (33) we see that the probability to find the electron at the points $\pm\boldsymbol{\alpha}_0$ decreases inversely proportionally to $\alpha_0$.

Using Eq. (33) in Eq.(11) gives the (averaged) angular-dependent multiphoton ionization decay rate in the ultrastrong-field limit

$$\frac{d\Gamma_n^{\mathrm{av}}}{d\Omega} \simeq \frac{|u(0)|^2\omega^2}{2\pi n^2 I\cos\theta}. \tag{34}$$

Here we have used the relation $k_n \simeq \sqrt{2n\omega}$ (where we have used $k_n = \sqrt{2[E(\alpha_0)+n\omega]}$ and we have invoked our condition of high frequency) and we have set $\alpha_0 = I^{1/2}\omega^{-2}$. Note the particularly simple way in which the angular-dependent decay rate depends on the intensity, the frequency, and the number of photons absorbed. It is, however, not possible to draw conclusions from this about the dependence of the (partial or total) angular-integrated multiphoton ionization decay rates on the intensity, the frequency, and the number of photons absorbed, since angular integration of Eq. (34) leads to divergence (for $\theta$ tends to 90°).

When making use of the scaling relation Eq. (31) in Eq. (28), we can show after some elementary manipulations, which we will not reproduce here, that

$$\Delta_n \simeq -\tfrac{2}{3}\ln\alpha_0 - \ln 2 + \mathcal{C}, \tag{35}$$

up to terms vanishing in the limit $\alpha_0 \to \infty$. In this formula we have defined the constant $\mathcal{C}$ by

$$\mathcal{C} = \mathcal{C}_1 + \mathcal{C}_2 = \int_0^1 \frac{|u(-\mathbf{e}\xi)|^2 - |u(0)|^2}{|u(0)|^2\xi}d\xi + \int_1^\infty \frac{|u(-\mathbf{e}\xi)|^2}{|u(0)|^2\xi}d\xi. \tag{36}$$

In the ultrastrong-field limit, we find for the partial multiphoton ionization decay rates $\Gamma_n$

$$\Gamma_n = \frac{\omega^2}{n^2 I}\left[A_1 \ln\left(\frac{n^3 I}{\omega}\right) + A_2\right]. \tag{37}$$

This relation was obtained from Eq. (26) by invoking Eq. (35) for $\Delta_n$, setting $\alpha_0 = I^{1/2}\omega^{-2}$, and replacing $k_n$ by $\sqrt{2n\omega}$. In Eq. (37) the constants $A_1$ and $A_2$ are given by

$$A_1 = \tfrac{1}{3}|u(0)|^2 \tag{38}$$

and

$$A_2 = |u(0)|^2[\ln 2 - 2\psi(\tfrac{1}{2}) + 2\mathcal{C}], \tag{39}$$

respectively. [Recall that Eq. (37) is valid for values of the intensity and frequency that fulfill our three above-mentioned conditions $\omega \gg |E_0(\alpha_0)|$, Eq. (7), i.e., $\alpha_0 k_n \gg 1$, and Eq. (29); i.e., $\alpha_0 \gg 1$.]

From Eq. (37) we find that in ultrastrong fields the *branching ratios* for decay by absorption of the various number of photons possible are only weakly dependent on the values of the intensity and frequency of the laser field, a situation that is in strong opposition to what happens in weak fields. From Eq. (37) we see that the rate of decay by multiphoton ionization depends on the number of photons absorbed, roughly through $n^{-2}$. Consequently, single-photon decay is dominant, while decay by more than one photon becomes gradually less important as the number of excess photons increases. However, if this number grows, the ratio of decay by absorption of $n$ to $n+1$ photons approaches unity. Due to this long-tail behavior in ultrastrong fields, excess-photon ionization (EPI) does nevertheless constitute a sizable part of the decay modes of the atom.

The peak pattern in the energy spectrum of photoelectrons that our theory predicts (for the case of an "ideal EPI experiment") differs drastically from what is predicted by LOPT, in weak fields. According to LOPT, the partial decay rates depend on the intensity through the number of photons absorbed via the well-known power law $\Gamma_n \propto I^n$. Furthermore, the partial decay rates drop with increasing frequency with a steeper and steeper slope as the number of photons absorbed increases (under the condition that the frequency is large with respect to the ionization potential). Consequently, in weak fields the peak pattern of EPI electrons is quite sensitive to the intensity and frequency of the irradiated light. Experiments carried out at higher intensities prove that this trend persists even beyond the limit where LOPT is applicable (see, e.g., [22,23]). This sensitivity of the peak pattern contrasts with the weak dependence which appears in our case.

The total multiphoton ionization decay rate $\Gamma$ can be easily obtained from Eq. (37) by summing over all open channels ($\Gamma = \sum_{n=1}^{\infty}\Gamma_n$). This gives

$$\Gamma = \frac{\omega^2}{I}\left[B_1 \ln\left(\frac{I}{\omega}\right) + B_2\right], \tag{40}$$

in which the constants $B_1$ and $B_2$ are defined by

$$B_1 = \frac{\pi^2}{18}|u(0)|^2 \tag{41}$$

and

$$B_2 = \frac{\pi^2}{6}|u(0)|^2[\ln 2 - 2\psi(\tfrac{1}{2}) + 2\mathcal{C}] - |u(0)|^2\zeta'(2), \tag{42}$$

respectively. As usual, $\zeta(z)$ denotes the Riemann zeta function, defined by $\zeta(z) = \sum_{n=1}^{\infty} n^{-2}$; in particular we have $\zeta(2) = \sum_{n=1}^{\infty} n^{-2} = \pi^2/6$ and $\zeta'(2) = -\sum_{n=1}^{\infty} n^{-2}\ln n = -0.937\,548\,254\,318\,5$. [$\psi(\frac{1}{2}) = -1.963\,510\,026\,021$.] [We remark that Eq. (40) is valid for values of the intensity and frequency that satisfy the three above-mentioned conditions.]

Equation (40) represents an important result. It shows how the lifetime of atomic hydrogen depends on the fre-

quency and the intensity under conditions that the intensity reaches extremely high values. We have found a striking feature: At high intensities, the hydrogen atom tends to stabilize at fixed, but otherwise arbitrarily chosen frequency. In fact, the lifetime of the atom increases practically proportionally to the intensity of the laser field, at fixed high frequency. From LOPT one finds that at low intensity, the ionization rate increases with the intensity if the frequency is kept fixed. (If the minimum number of photons to ionize the atom is $n$, this increase is proportional to the $n$th power of the intensity.) Consequently, if at fixed frequency the intensity is increased from the value zero, the lifetime of the atom first decreases, then reaches one or, possibly, more minima, and subsequently, within the general assumptions of our theory, increases monotonically with no bound. It is important to be aware of the possibility that the lifetime of the atom is not a unimodal function of the intensity. This situation may occur, when at low intensities we start off with a frequency smaller than the field-free ionization potential, so that, as the intensity is increased, atomic levels, displaced by the (intensity-dependent) ac Stark effect, shift into resonance. As has recently been found, these resonances can also occur with atomic levels that disappear when the intensity is lowered ("field-induced bound states"). These states arise from so-called shadow states: eigensolutions of the Floquet-system with "wrong" asymptotic boundary conditions (ingoing instead of outgoing waves) [24].

The unexpected (relative) stability of the hydrogen atom in ultrastrong fields can be understood qualitatively on the basis of the following approximation to the *open-channel part* of the decaying state of the atom in the field [see Eqs. (64) and (65) of paper I]:

$$\tilde{\Psi}(\mathbf{r},t) = \int d\mathbf{r}' \int dt' \mathcal{G}_0^{(+)}(\mathbf{r},\mathbf{r}',t-t')\rho(\mathbf{r}',t'), \tag{43}$$

in which the source density $\rho(\mathbf{r},t)$ is given by

$$\rho(\mathbf{r},t) = -\frac{\Phi(-\boldsymbol{\alpha}(t))\exp(-iWt)}{|\mathbf{r}+\boldsymbol{\alpha}(t)|}. \tag{44}$$

As Eq. (43) demonstrates, the decaying state consists of a superposition of outgoing electron waves (corresponding to the ionization process) which are created by the source of Eq. (44). It shows that (in the Kramers frame of reference) outgoing electron waves are created in the vicinity of the momentary position of the oscillating proton. The calculation of the multiphoton ionization amplitude from Eqs. (43) and (44) yields exactly our simplified expression, Eq. (1). This latter expression contains the probability amplitude $\Phi(-\boldsymbol{\alpha}(\phi))$ to find the electron at the position of the proton and a phase factor $\exp\{i\boldsymbol{\alpha}(\phi)\cdot\mathbf{k}_n\}$ associated with the displacement of the proton from the origin of the Kramers reference frame by $-\boldsymbol{\alpha}(\phi)$. These notions form the key to the physical mechanism underlying the stabilization of the atom in ultrastrong fields, which we will now discuss. The first stabilizing effect arises from the phenomenon of radiative distortion of the electron cloud, as discussed in Ref. [2]. This causes the probability amplitude of finding the electron at the position of the proton to decrease with increasing $\alpha_0$ (or at fixed frequency, with increasing intensity). On the other hand, in the ultrastrong-field limit, the de Broglie wavelengths of the photoelectrons are small with respect to the spatial extension ($2\alpha_0$) of the source from which they are emitted, as follows from the condition Eq. (7), i.e., $\alpha_0 k_n \gg 1$. It thus follows that the phase factor $\exp[i\boldsymbol{\alpha}(\phi)\cdot\mathbf{k}_n]$ varies rapidly with the phase $\phi$ of the field. Consequently, waves emitted from different positions of the proton tend to cancel each other due to destructive interference. This suppresses the outgoing flux of electrons with increasing $\alpha_0$ (or at fixed frequency, with increasing intensity). Since our arguments for "high-intensity stabilization" are based on Eqs. (43) and (44), which do not pertain to a particular state of polarization, the phenomenon of high-intensity stabilization is universal. Clearly, the precise dependence of the total decay rate on the intensity depends on the details of its two underlying mechanisms, namely "radiative distortion of the electron cloud" and "destructive interference of the outgoing electron waves" [25]. Note that high-intensity stabilization sets in when Eq. (17) is satisfied. (Compare Dörr *et al.* [24]) and that radiative distortion assists, but is not necessary for stabilization (see Sec. II B).

Equation (40) presents another surprise. As Eq. (40) shows, the total ionization decay rate is approximately proportional to the square of the frequency. This demonstrates that in the extreme case of ultrastrong fields, the lifetime of the atom increases substantially with decreasing frequency. This is in strong contrast with what we find from LOPT. According to LOPT, at low intensities and high frequencies, the lifetime of the atom increases substantially when the frequency is increased. For single-photon ionization we have the well-known $\omega^{-9/2}$ decay of the ionization decay rate with increasing frequency [see Eq. (42) of paper I ], whereas it can be argued that this decrease is even steeper if the excess number of absorbed photons is larger.

The frequency and intensity dependence of the total decay rate given by Eq. (40) implies that for frequencies that are low, yet sufficiently high so as to meet the three conditions under which they are valid, the lifetime of the hydrogen atom in an ultrastrong radiation field can be quite moderate. This will be discussed in detail in Sec. III C.

## III. NUMERICAL RESULTS AND DISCUSSION

In this section we will present and discuss our numerical results of the decay rates for multiphoton ionization from the ground state of atomic hydrogen in a superintense, high-frequency laser field of linear polarization. Our calculations are based on expression Eq. (2) for the $n$-photon ionization amplitude $f_n$. The coefficients $\Phi_m$ in this expression are defined in Eq. (3).

The form of Eq. (2) is well suited for numerical evaluations. For a given value of $\alpha_0$, we determine the coefficients $\Phi_m$ by quadrature

$$\Phi_m = \frac{1}{2\pi}\int_{-\pi}^{+\pi} e^{im\phi}\Phi(-\boldsymbol{\alpha}_0\cos\phi)d\phi$$
$$= \frac{2}{\pi}\int_0^{\pi/2} \cos(m\phi)\Phi(\boldsymbol{\alpha}_0\cos\phi)d\phi \tag{45}$$

for $m$ even and zero for $m$ odd, up to a value $M$, which we choose sufficiently large. [The wave function $\Phi(\mathbf{r})$ was obtained in Ref. [2].] In Eq. (45) we have made use of the fact that the ground state has parity $P = 0$. The insertion of these coefficients into Eq. (2) then immediately yields the multiphoton ionization amplitude $f_n$. The momenta $k_n$ are computed from $k_n = \sqrt{2[E_0(\alpha_0) + n\omega]}$ with the values $E_0(\alpha_0)$ given in Ref. [2] ([26]).

In Sec. III A we study the angular distributions of the photoelectrons. In Sec. III B we discuss the (angle-integrated) partial rates as a function of the number of photons absorbed. Finally, in Sec. III C we present our results for the total ionization decay rates of the atom.

The validity of our approach is limited by the requirement of high frequency $\omega \gg |E_0(\alpha_0)|$. We have studied those cases in which the frequency is at least a factor of 4 higher than the binding potential of the atom in the field. Under similar conditions, as has been shown by Bardsley and Comella and by Bhatt, Piraux, and Burnett using a direct numerical computation on one-dimensional model atoms, the exact results compare reasonably well with the lowest-order results provided by the Gavrila-Kaminski theory [27]. Thus the above condition poses a lower limit to the values of the frequency that we can consider. Moreover, in all cases we have to ensure that $\Gamma \ll \omega$ in order that our approach of stationary decay is applicable. Yet we have chosen the frequency such that it is not unrealistically high. (The maximum value we have chosen is $\omega = 1$ a.u., the minimum value is $\omega = 0.125$ a.u.)

On the other hand, the assumption that relativistic and retardation effects can be neglected also imposes certain restrictions on the values of $\alpha_0$ and $\omega$ for which our approach is valid. Relativistic effects become important when the maximum jitter velocity of a classical free-electron driven by the field ($= \alpha_0\omega$) becomes comparable to the speed of light ($c \approx 137$ a.u.). The validity of the dipole approximation requires the wavelength of the light to be large compared to the size of the atom. The estimation of the size of the atom in the laboratory frame of reference by $4\alpha_0$ leads to essentially the same restriction, as one can easily check.

With the above restrictions, we are able to treat the entire intensity range which extends from 1 to $10^4$ atomic units of intensity. This includes the interesting frequency and intensity values of the pulses created by laser systems which are already in operation, but extends beyond into the intensity range of the near-future generation of laser systems which is now being developed in laboratories throughout the world [28].

### A. Angular-dependent multiphoton ionization decay rates

As well known, in the case of linear polarization, the angular-dependent distributions of ejected electrons possess axial symmetry with respect to the polar axis and are also invariant under a reflection in the origin. Consequently, it suffices to present our results for $d\Gamma_n/d\Omega$ as a function of the polar angle ranging from 0° to 90°.

In Figs. 1–3 we present some representative cases. In Figs. 1–3 we have plotted the cases $\alpha_0 = 20, \omega = 0.25$; $\alpha_0 = 20, \omega = 1$; and $\alpha_0 = 100, \omega = 0.125$, respectively. In all three figures we have displayed the results for ionization by absorption of one, two, and three photons, respectively. As is apparent from these figures we find in agreement with Eq. (10) regular oscillations between zero and an envelope which varies smoothly with the polar angle. As was predicted in Sec. II A we find that the overall behavior of the photoelectrons is to be ejected in directions away from the polarization direction. The interference oscillations become more rapid the higher the value of $\alpha_0$, $\omega$, or $n$ (the number of photons absorbed). As one can easily check, the number of interference fringes between

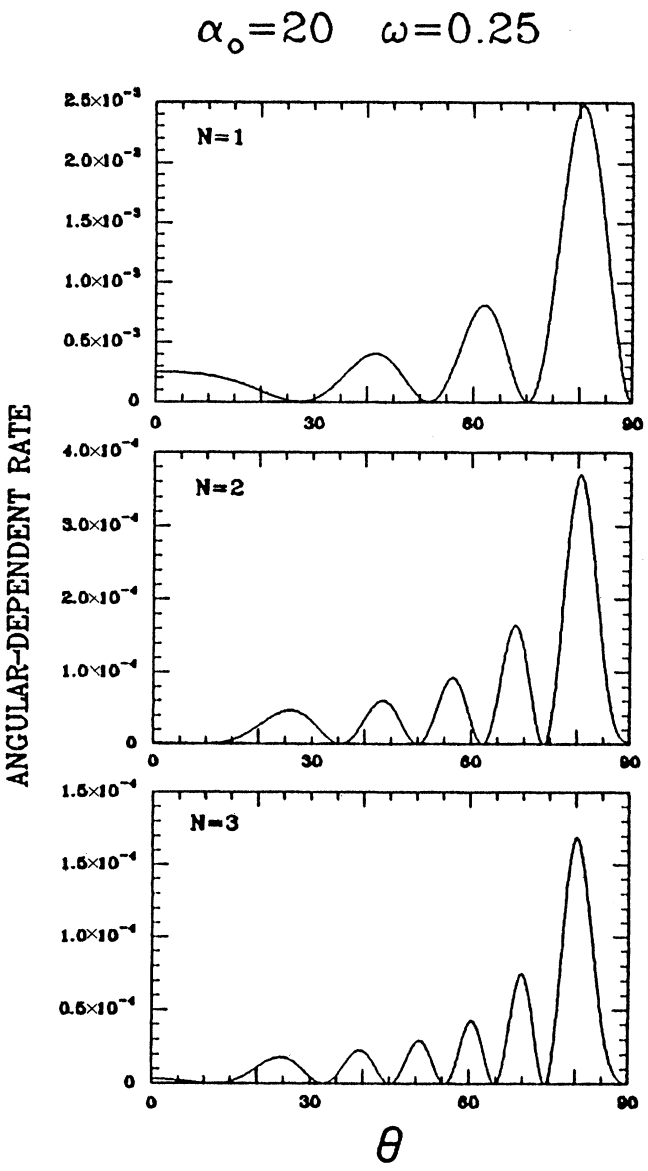


FIG. 1. Angular-dependent decay rates for absorption of one, two, and three photons, respectively, for ionization from the ground state of atomic hydrogen in a superintense, linearly polarized laser field (of $\alpha_0 = 20$ and $\omega = 0.25$), as a function of the polar angle (in atomic units).

0° and 90° is indeed approximately equal to $\alpha_0 k_n/\pi$ as noted in Sec. II A. For example, for the case of ionization by absorption of three photons in a field of $\alpha_0 = 20$ and $\omega = 1$, we have $\alpha_0 k_3/\pi = 15.8$, whereas by inspection of Fig. 2 we find approximately 14.5 oscillations. Note also that, as we have predicted, the width of the fringes becomes smaller as the angle with the polarization axis is increased. From Figs. 1–3 we may remark that in accordance with Eq. (63) of paper I $d\Gamma_n/d\Omega$ vanishes for $\theta = 90°$ if the number of photons absorbed is odd, whereas it attains a finite value for even $n$. (This is most clearly shown in Fig. 3. As it turns out, the values of the partial decay rate for $\theta = 90°$ and $n = 2$ in Figs. 1 and 2 are rather small.)

In Fig. 4 we make a comparison to Eq. (10), which is valid for $|\alpha_0 \cdot \mathbf{k}_n| \gg 1$, for the case of three-photon absorption in a field of $\alpha_0 = 20$ and $\omega = 1$. As expected, the agreement is better for small values of the polar angle and becomes gradually worse if the direction perpendicular to the polarization axis is approached. (Although $\alpha_0 k_n = 49.6 \gg 1$, as the polar angle approaches 90°, the condition $\alpha_0 \cdot \mathbf{k}_n \gg 1$ is no longer fulfilled.) For smaller values of $\alpha_0 k_n$ (not shown), the absolute comparison of Eq. (10) with Eq. (2) is not as good, but nevertheless

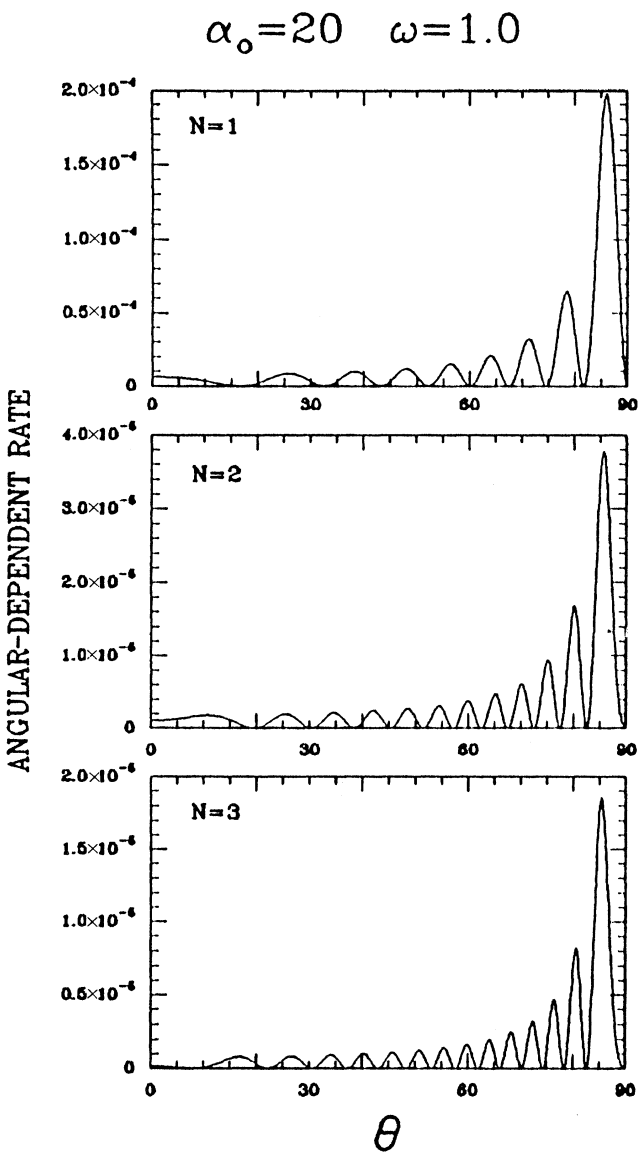


FIG. 2. Angular-dependent decay rates for absorption of one, two, and three photons, respectively, for ionization from the ground state of atomic hydrogen in a superintense, linearly polarized laser field (of $\alpha_0 = 20$ and $\omega = 1.0$), as a function of the polar angle (in atomic units).

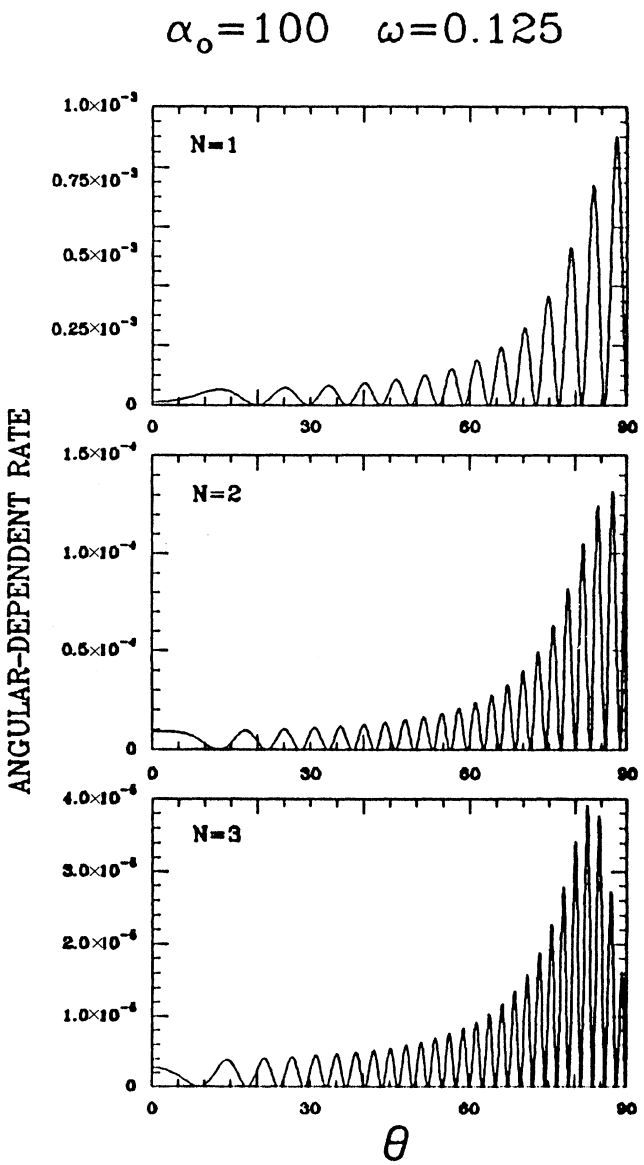


FIG. 3. Angular-dependent decay rates for absorption of one, two, and three photons, respectively, for ionization from the ground state of atomic hydrogen in a superintense, linearly polarized laser field (of $\alpha_0 = 100$ and $\omega = 0.125$), as a function of the polar angle (in atomic units).

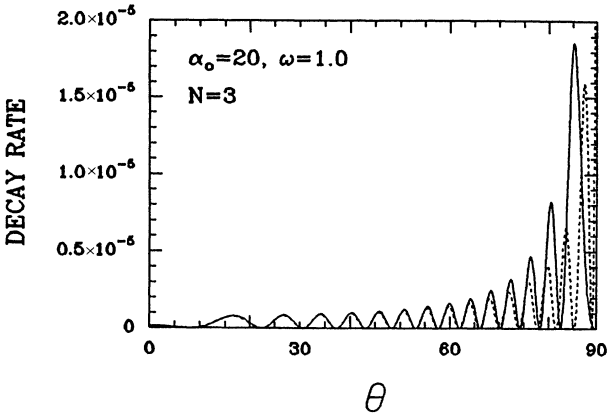


FIG. 4. Comparison of the angular-dependent decay rate obtained from Eq. (2) (solid curve) with Eq. (10) (dotted curve) for ionization by three-photon absorption from the ground state of atomic hydrogen in a superintense, linearly polarized laser field (of $\alpha_0 = 20$ and $\omega = 1$), as a function of the polar angle (in atomic units).

reproduces the positions of the maxima and minima in the angular-dependent rate [see Eqs. (14) and (15)] surprisingly well.

### B. Angular-integrated multiphoton ionization decay rates

Before discussing in Sec. III C the lifetime of the atom decaying by multiphoton ionization, let us first study the partial decay rates as a function of the number of photons absorbed. Our results are summarized in Tables I–IV, where we have given the partial decay rates for ionization by absorption of one through five photons for $\omega = 1.0, 0.5, 0.25$, and 0.125, respectively. (In the tables we have put powers of 10 in between square brackets.) These values were computed by numerical integration of the angular-dependent rates obtained directly from Eq. (2). Typical cases are illustrated in Figs. 5–7, where we have given a graphical representation of the partial decay rates as a function of the number of photons absorbed for $1 \leq n \leq 10$. We have chosen the same examples for which we have presented the angular-dependent rates in Sec. III A. These figures can be looked upon as the peak pattern obtained in an ideal EPI experiment in which the photoelectron yield is recorded as a function of the energy [29].

As is apparent, the single-photon decay channel is dominant, and the heights of the higher-order peaks decrease steadily with their order. Yet for higher orders, two consecutive peaks in the EPI spectrum attain similar heights. Because of this long-tail behavior, the ratio of decay by excess-photon ionization to single-photon ionization is still quite significant. For example, for $\alpha_0 = 20$ and $\omega = 1$ the decay rate for absorption up through ten photons equals $\Gamma = 0.000\,420$ (from Table VI), whereas decay by single-photon absorption yields $\Gamma_1 = 0.000\,298$ (see Table I). Consequently, about one-third of the decay takes place by excess-photon ionization. We also find, when comparing the various cases represented in Figs. 5–7, that the pattern of peaks is only weakly dependent on the intensity and the frequency. These notions agree well with the analysis presented in Sec. II C [although strictly spoken, the validity of our expression (37) is limited to ultrastrong fields].

In Table V, we give the values of $|\Phi(\alpha_0)|$ and $\Delta_n$ ($n \leq 5$) for various values of the parameter $\alpha_0$. Here we have calculated $\Delta_n$ by the evaluation of the sum $S_n^{(2)}$ of Eq. (23) and using the relation $\Delta_n = S_n^{(2)}/|\Phi(\alpha_0)|^2$ [see Eq. (27)]. With the values of $|\Phi(\alpha_0)|^2$ and $\Delta_n$ given in Table V, the partial decay rates $\Gamma_n$ can be calculated from Eq. (26) for arbitrary values of the frequency subject to the conditions $\alpha_0 k_n \gg 1$ and $\omega \gg |E_0(\alpha_0)|$. Excellent agreement is obtained with Eqs. (26) and (28) for almost all cases that we have investigated (summarized in Table VI and Fig. 8 of Sec. III C). For example, for the cases $\alpha_0 = 100$ and $\omega = 0.125$ and $\alpha_0 = 20$ and $\omega = 1$, direct numerical integration from Eq. (2) agrees with Eq. (26) in three significant figures [for all values of $n$ in Table V ($1 \leq n \leq 5$)]. For lower values of $\alpha_0 k_n$, the agreement is not as good. For example, for single-photon ionization in a field of $\alpha_0 = 20$ and $\omega = 0.25$ we obtain by direct calculation from Eq. (2) $\Gamma_1 = 0.007\,44$ (see Table III), while Eq. (26) yields $\Gamma_1 = 0.007\,60$ (see Table V).

### C. Total multiphoton ionization decay rates

Our results for the total decay rates for multiphoton ionization from the ground state of atomic hydrogen in a superintense, linearly polarized laser field, as a function of the intensity, are given in Table VI for various

TABLE I. Values of partial decay rates $\Gamma_n$ for ionization by absorption of one through five photons, from the ground state of atomic hydrogen in a superintense, linearly polarized laser field of $\omega = 1$ a.u., as a function of $\alpha_0$ (in atomic units). $a[b] = a \times 10^b$.

| $\alpha_0$ | $\Gamma_1$ | $\Gamma_2$ | $\Gamma_3$ | $\Gamma_4$ | $\Gamma_5$ |
|---|---|---|---|---|---|
| 5 | 1.08[−2] | 2.25[−3] | 9.27[−4] | 4.91[−4] | 3.01[−4] |
| 10 | 1.44[−3] | 3.17[−4] | 1.38[−4] | 7.52[−5] | 4.71[−5] |
| 20 | 2.98[−4] | 5.56[−5] | 2.52[−5] | 1.42[−5] | 8.92[−6] |
| 40 | 1.17[−4] | 2.02[−5] | 7.92[−6] | 4.57[−6] | 2.96[−6] |
| 70 | 4.63[−5] | 8.95[−6] | 3.27[−6] | 1.76[−6] | 1.15[−6] |
| 100 | 2.13[−5] | 4.28[−6] | 1.54[−6] | 7.98[−7] | 5.20[−7] |

TABLE II. Values of partial decay rates $\Gamma_n$ for ionization by absorption of one through five photons, from the ground state of atomic hydrogen in a superintense, linearly polarized laser field of $\omega = 0.5$ a.u., as a function of $\alpha_0$ (in atomic units).

| $\alpha_0$ | $\Gamma_1$ | $\Gamma_2$ | $\Gamma_3$ | $\Gamma_4$ | $\Gamma_5$ |
|---|---|---|---|---|---|
| 10 | 7.20[−3] | 1.36[−3] | 5.62[−4] | 3.00[−4] | 1.85[−4] |
| 20 | 1.34[−3] | 2.24[−4] | 9.93[−5] | 5.54[−5] | 3.44[−5] |
| 40 | 4.91[−4] | 7.88[−5] | 3.00[−5] | 1.72[−5] | 1.11[−5] |
| 70 | 1.87[−4] | 3.45[−5] | 1.23[−5] | 6.58[−6] | 4.30[−6] |
| 100 | 8.53[−5] | 1.66[−5] | 5.81[−6] | 2.98[−6] | 1.94[−6] |
| 200 | 2.02[−5] | 4.34[−6] | 1.60[−6] | 7.73[−7] | 4.68[−7] |

values of the frequency. The values for the total multiphoton ionization decay rates were obtained by summing the partial rates $\Gamma_n$ for single- through ten-photon absorption. To facilitate their discussion, we have displayed them graphically in Fig. 8, where we have also indicated the corresponding values of the parameter $\alpha_0$. In Fig. 8 the intensity ranges from 1 to $10^4$ a.u. and the frequency values we have considered are 0.125, 0.25, 0.5, and 1.0 a.u. Because of the several orders of magnitude over which both the intensity and the total multiphoton ionization decay rate vary, we have chosen a representation with a double-logarithmic division.

The four dotted curves in Fig. 8 (which appear to be quasistraight on the log-log scale) represent the result of Eq. (40) for $\omega = 1.0, 0.5, 0.25$, and 0.125, respectively. The values of the constants $B_1$ and $B_2$ in Eq. (40) were extracted from the values of the ground-state wave function on the line segment of charge for $\alpha_0 = 1000$. We thus obtain [30]

$$B_1 = 0.007\,46, \qquad B_2 = 0.285. \tag{46}$$

Although Eq. (40) strictly holds for the ultrastrong-field regime, it nevertheless forms a suitable basis from which we can discuss the overall dependence of the total decay rates on the frequency and the intensity.

As is apparent from Fig. 8, markers corresponding to the same value of the frequency follow approximately the dotted curves. As one can easily check, the quasistraight lines have a slope of about $-1$. This demonstrates that at fixed frequency and increasing intensity, the total multiphoton ionization decay rate *decreases* roughly inversely proportionally to the intensity, in agreement with Eq. (40). This is the (*a priori* unexpected) high-intensity stabilization as discussed in Sec. II C of this paper.

The values of the frequency that we have represented in Fig. 8, namely 0.125, 0.25, 0.5, and 1, respectively, were chosen in a geometric progression. As Fig. 8 displays, the quasistraight curves representing the result of Eq. (40) are approximately equidistant, which reflects the fact that the total ionization decay rate at a fixed value of the intensity depends on the frequency through a power law. Indeed, it follows from Eq. (40) that (at fixed intensity) the total multiphoton ionization decay rate is roughly proportional to the square of the frequency. This can be easily checked by inspection of Fig. 8, where we find that, when at fixed intensity the frequency is decreased by a factor of 2, the total decay rate decreases by about a factor of 4. As we have already discussed in Sec. II C, the dependence of the total multiphoton ionization decay rate on the intensity and the frequency under these extreme radiation conditions is totally different from what is obtained from LOPT, valid for low intensities. Indeed, according to LOPT the total decay rates *increase* rather than *decrease* with increasing intensity at fixed frequency. Moreover, according to LOPT the total decay rates *decrease* rather than *increase* with *increasing* frequency, at fixed (low) intensity.

From Fig. 8 we may also remark that markers corresponding to the same value of $\alpha_0$ (e.g., 20, 40, 70, 100, and 200) also lie on almost straight lines. As was noted from Eq. (26) in Sec. II B, at a fixed value of $\alpha_0$, the (partial) decay rates drop approximately with the square

TABLE III. Values of partial decay rates $\Gamma_n$ for ionization by absorption of one through five photons from the ground state of atomic hydrogen in a superintense, linearly polarized laser field of $\omega = 0.25$ a.u., as a function of $\alpha_0$ (in atomic units).

| $\alpha_0$ | $\Gamma_1$ | $\Gamma_2$ | $\Gamma_3$ | $\Gamma_4$ | $\Gamma_5$ |
|---|---|---|---|---|---|
| 20 | 7.44[−3] | 9.76[−4] | 4.08[−4] | 2.22[−4] | 1.35[−4] |
| 40 | 2.30[−3] | 3.18[−4] | 1.17[−4] | 6.62[−5] | 4.22[−5] |
| 70 | 8.10[−4] | 1.37[−4] | 4.68[−5] | 2.47[−5] | 1.61[−5] |
| 100 | 3.61[−4] | 6.52[−5] | 2.22[−5] | 1.12[−5] | 7.25[−6] |
| 200 | 8.23[−5] | 1.70[−5] | 6.11[−6] | 2.91[−6] | 1.75[−6] |
| 400 | 2.12[−5] | 4.79[−6] | 1.83[−6] | 9.02[−7] | 5.15[−7] |

TABLE IV. Values of partial decay rates $\Gamma_n$ for ionization by absorption of one through five photons from the ground state of atomic hydrogen in a superintense, linearly polarized laser field of $\omega = 0.125$ a.u., as a function of $\alpha_0$ (in atomic units).

| $\alpha_0$ | $\Gamma_1$ | $\Gamma_2$ | $\Gamma_3$ | $\Gamma_4$ | $\Gamma_5$ |
|---|---|---|---|---|---|
| 70 | 4.14[−3] | 5.79[−4] | 1.84[−4] | 9.48[−5] | 6.10[−5] |
| 100 | 1.73[−3] | 2.71[−3] | 8.68[−5] | 4.25[−5] | 2.74[−6] |
| 200 | 3.59[−4] | 6.85[−5] | 2.37[−5] | 1.11[−5] | 6.55[−6] |
| 400 | 8.79[−5] | 1.87[−5] | 7.18[−6] | 3.43[−6] | 1.91[−6] |
| 1000 | 1.37[−5] | 3.24[−6] | 1.34[−6] | 6.81[−7] | 3.93[−7] |

of the frequency, if the latter is increased. [We do not need $\alpha_0$ to be high, as in Eq. (40), in order that Eq. (26) be valid.] This simply illustrates the high-frequency stabilization which forms the central issue of the Gavrila-Kaminski iteration scheme. It thus follows that at fixed $\alpha_0$, i.e., for a given distortion of the atom, the total decay rate *decreases* with the square root of the intensity as the latter is increased. Consequently, markers corresponding to the same value of the parameter $\alpha_0$ appear in Fig. 8 on straight lines with a slope of $-0.5$, as one can easily check.

We could compare our calculations with one published very recently by Walet, using a novel approach, solving the Floquet equations in the Kramers frame of reference on a grid, using a variant of complex rotation which is most suitable to the case of interest. In this paper preliminary results are presented only for $\alpha_0 = 20$ (see his Fig. 9). For $\omega = 0.5$, our results presented in Fig. 8 show only 20% deviation from his data [31].

As is apparent from Fig. 8, the lifetime is extremely short for values of the intensity about the atomic unit, which could have been expected from extrapolation of the well-known LOPT formula for single-photon ionization towards high intensities. (Although one has to be very careful with such estimates, since as was shown in Ref. [32] perturbation theory may overestimate decay rates at intermediately high intensities by several orders of magnitude.) However, for low enough frequencies and very high intensities, we find from Fig. 8 that the lifetime of the atom can be remarkably long. For example, for $I = 100$ and $\omega = 0.25$, values that have already been announced [33], the width of the decaying state is only $2 \times 10^{-4}$. This amounts to about one-seventeenth of the interlevel distance and corresponds to about 200 oscillations of the oscillating light field (i.e., 120 fs). (The atomic unit of time amounts to $\tau_0 = 0.0242$ fs.)

## IV. EXPERIMENTAL CONSEQUENCES: DISCUSSION

In the foregoing, we established the existence of radiation dressed states of the atom in fields of intensities far beyond the atomic unit, which have lifetimes that allow—at least in principle—experimental proof of their existence. In the following we would like to discuss how it might be possible to verify the existence of these (strongly) deformed states.

Observation of the dressed *ground state*, starting from the atom outside the field in the ground state, appears to be difficult to realize. As we have shown in Sec. III,

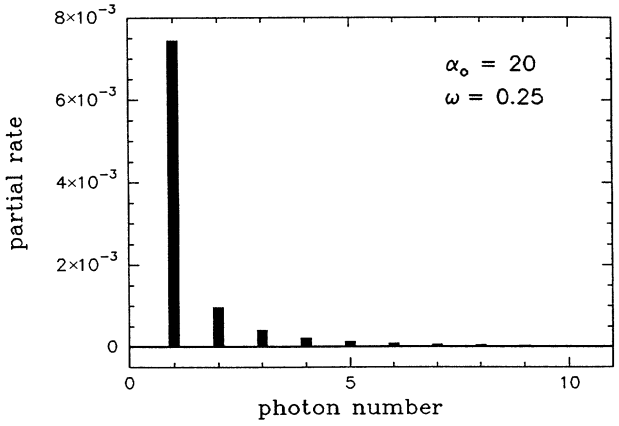


FIG. 5. Partial decay rates for ionization from the ground state of atomic hydrogen in a superintense, linearly polarized laser field (of $\alpha_0 = 20$ and $\omega = 0.25$), as a function of the number of photons absorbed (in atomic units).

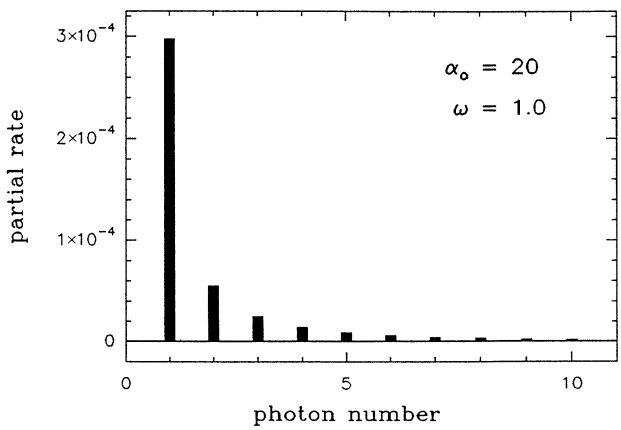


FIG. 6. Partial decay rates for ionization from the ground state of atomic hydrogen in a superintense, linearly polarized laser field (of $\alpha_0 = 20$ and $\omega = 1.0$), as a function of the number of photons absorbed (in atomic units).

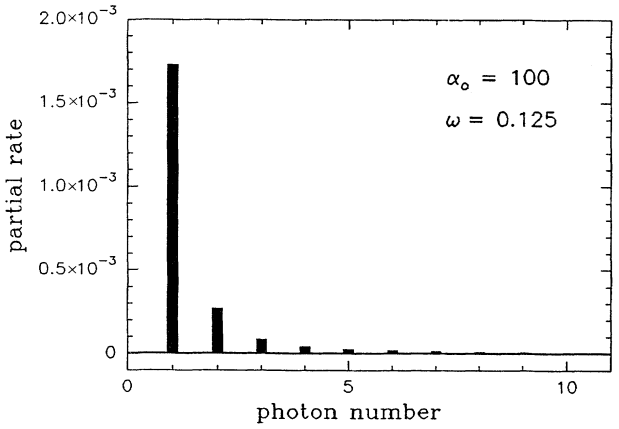


FIG. 7. Partial decay rates for ionization from the ground state of atomic hydrogen in a superintense, linearly polarized laser field (of $\alpha_0 = 100$ and $\omega = 0.125$), as a function of the number of photons absorbed (in atomic units).

during the buildup of the field intensity, the atom in its ground state is very short lived, even for the soft-x-ray laser systems that are now being developed (see Ref. [34]). The atom is likely to be ionized in the edges of the pulse before it sees the very high intensities (see also [35]). A sudden rise of the intensity ("square" intensity profile of the pulse or relativistic atomic beam) does not seem to solve this difficulty, not to mention the problems arising from transient effects that will thus be induced in the atom. These transient effects will mask the spectrum of the atom dressed by the very intense field that we want to resolve. The fact that one cannot appeal to the conventional experimental methods is apparently the price one has to pay for the curiosity to learn about the atomic dynamics in superintense fields. In the following, we will outline a few alternative schemes that one may envisage. Let us for the moment postpone the discussion of the ground state and examine whether the consideration of excited states can offer a solution to this problem.

The situation is indeed different for *Rydberg states* of high magnetic quantum number. These may be prepared outside the field, starting from the atom in its ground state, e.g., with the help of an excitation laser of circular polarization. In the first place, the frequency condition that requires the photon energy to be much larger than the binding energy can be fulfilled rather easily (in principle, even with lasers operating in the infrared; see Ref. [2]). In contrast to the ground state, this can be done before the atom has entered the field, i.e., before its ionization potential has been reduced by the intense field. In the second place, it is expected that the lifetime of these states can be made sufficiently large so as to survive the (high) intensities, which are present during the rise of the pulse, simply by increasing the magnetic quantum number $m$ [36]. There are, however, some limitations. One has to take care that—taking into consideration the high principal quantum number—the size of the excited state does not get so large that the dipole approximation breaks down. For example, one cannot have $n = 100$ and at the same time $\omega = 0.1$, or larger. Another point that we have to keep in mind is that, in order to create interesting effects of "radiative distortion," we need $\alpha_0$ to be high with respect to the size of the unperturbed state (see Ref. [2]). Thus the value of $\alpha_0$ that we need in order to achieve a significant distortion of our Rydberg state must be quite large, much larger than for the ground state. (For excited states, however, fields of relatively low frequency can be considered, so that it is not difficult for a given intensity to obtain large values of $\alpha_0$.)

On the other hand, as we learned from the preceding sections, high-intensity stabilization can also be realized by creating a situation for which $\alpha_0^2\omega$ is large. This appears to be much easier to realize in practice. As we have discussed in Sec. II A, this condition defines what we have called the highly nonperturbative radiation regime. As we have pointed out, this radiation regime is characterized by destructive interference of electron waves emitted from different positions of the proton in the Kramers reference frame. It yields angular distributions of photoelectrons and a peak pattern in their energy spectrum that are entirely different from what is obtained in fields of moderately high intensity (see Secs. II and III).

So far we have been thinking of the preparation of a *pure state* outside the field which subsequently enters the pulse *adiabatically*. Yet there is another way in which excited states can be employed, namely in the form of a

TABLE V. Values of $|\Phi(\alpha_0)|$ and $\Delta_n$ ($n \leq 5$) for the ground state of atomic hydrogen in a superintense, linearly polarized laser field, as a function of $\alpha_0$ (in atomic units).

| $\alpha_0$ | $\lvert\Phi(\alpha_0)\rvert$ | $\Delta_1$ | $\Delta_2$ | $\Delta_3$ | $\Delta_4$ | $\Delta_5$ |
|---|---|---|---|---|---|---|
| 5 | 0.045 2 | −0.291 | −0.296 | −0.600 | −0.842 | −1.01 |
| 10 | 0.021 7 | +0.520 | +0.294 | +0.231 | +0.0568 | −0.128 |
| 20 | 0.014 1 | +0.443 | −1.15 | −1.09 | −1.15 | −1.33 |
| 40 | 0.012 6 | +0.0303 | −2.16 | −2.87 | −2.86 | −2.90 |
| 70 | 0.010 6 | −0.516 | −2.20 | −3.33 | −3.63 | −3.63 |
| 100 | 0.008 40 | −0.454 | −2.04 | −3.33 | −3.84 | −3.86 |
| 200 | 0.005 68 | −0.614 | −1.79 | −3.06 | −3.93 | −4.29 |
| 400 | 0.004 11 | −1.07 | −1.84 | −2.84 | −3.76 | −4.42 |
| 1000 | 0.002 61 | −1.64 | −2.07 | −2.70 | −3.42 | −4.12 |

TABLE VI. Values of total decay rates $\Gamma$ for multiphoton ionization from the ground state of atomic hydrogen in a superintense, linearly polarized laser field, as a function of $\alpha_0$ for various values of the frequency (in atomic units).

| $\alpha_0$ | $\omega = 0.125$ | $\omega = 0.25$ | $\omega = 0.5$ | $\omega = 1$ |
|---|---|---|---|---|
| 5 | | | | 1.53[−2] |
| 10 | | | 9.97[−3] | 2.11[−3] |
| 20 | | 9.45[−3] | 1.83[−3] | 4.20[−4] |
| 40 | | 2.93[−3] | 6.51[−4] | 1.59[−4] |
| 70 | 5.18[−3] | 1.07[−3] | 2.54[−4] | 6.39[−5] |
| 100 | 2.22[−3] | 4.82[−4] | 1.17[−4] | 2.96[−5] |
| 200 | 4.83[−4] | 1.14[−4] | 2.84[−5] | |
| 400 | 1.22[−4] | 3.03[−5] | | |
| 1000 | 2.01[−5] | | | |

Rydberg *wave packet*. (We shall continue to assume that the entrance of the atom into the laser pulse proceeds adiabatically.) This packet could be prepared outside the field, starting from the atom in its ground state with the help of a pulsed excitation laser of circular polarization, similarly as above. When the excitation laser pulse has passed, the packet moves out in an "orbit," whose recurrence time is essentially dictated by the laws of classical mechanics. After the orbit time ($\tau = 2\pi n^{-3}$, with $n$ the principal quantum number) the wave packet has returned near to its original position, i.e., close to the proton. If during this motion the wave packet is irradiated by an intense laser, appreciable ionization will take place only when it passes very closely to the proton. This simply reflects what we discussed in Sec. V of paper I, namely that it is only in the immediate vicinity of the proton that appreciable energy transfer to the electron can take place (see also [36]). This effect was demonstrated experimentally by ten Wolde *et al.* [37] by probing the atom with a second laser and recording the ionization signal as a function of time. The time-resolved ionization signal shows a series of peaks spaced by the round-trip time of the electron. For the case of their experiment (principal quantum number $n \approx 40$), this corresponded to a few picoseconds. By using now a very intense laser pulse instead of a weak probe pulse as was used in this experiment, it appears to be possible to synchronize the excitation pulse and the "probe" pulse in such a way that the packet, submerged in the relatively weak-field part of the pulse, has only a small probability to become ionized (where the wave packet is at a large distance from the nucleus), until it reaches the region where the intensity attains its peak value (where the wave packet is close to the nucleus). (Obviously the theory summarized in Sec. II of paper I applies to ionization from a stationary state and has to be modified accordingly so as to describe ionization from a wave packet.) It is important to realize that in order to draw interesting conclusions from this experiment, the lifetime of the atom needs to be long with respect to the round-trip time of the electron.

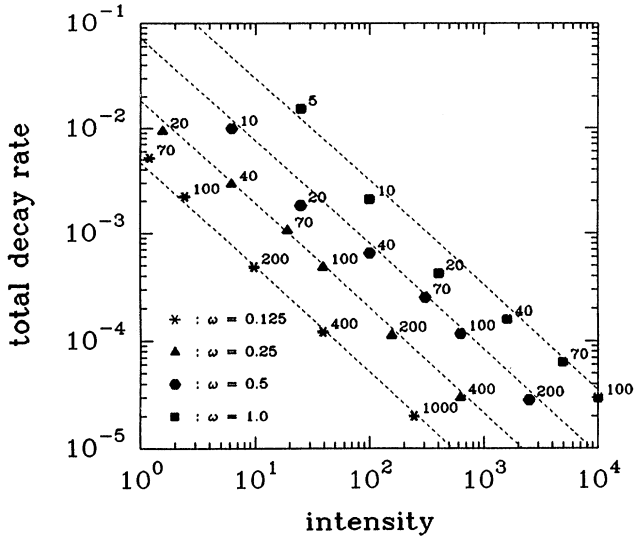


FIG. 8. Total decay rates for multiphoton ionization from the ground state of atomic hydrogen in a superintense, linearly polarized laser field, as a function of the intensity for various values of the frequency (in atomic units). The numbers next to the markers indicate the values of $\alpha_0$. The dotted curves represent the result of Eq. (40).

It will be clear from the above discussion that Rydberg states do offer an interesting alternative to the ground state for demonstrating nonperturbative effects of the interaction of the radiation field with the atom. In contrast to the ground state of the atom, which we have studied in detail in this work, at present no values for the lifetimes of Rydberg states are available and it is therefore difficult to substantiate to a larger extent than we have done above, the possible realization of an experiment in which the theory could be tested.

Let us now return to the discussion of an experiment in which the deformed ground state could be observed. When electrons are scattered from protons in the presence of an intense radiation field, the elastic-scattering cross section will exhibit deviations from the well-known Rutherford formula. In the case that the scattering is inelastic (i.e., involving the net absorption or emission of a certain number of photons) one speaks of "free-free

transitions." During the past few years much interest has developed in the study of this phenomenon. (For a review about this subject, see, e.g., [38] and [39]. For particular experiments carried out to study this phenomenon, see, e.g., Refs. [40, 41].) In fact, the basic formalism of the Gavrila-Kaminski theory was originally developed for these situations [42]. In this theory—to lowest order in the iteration—the electron is elastically scatttered from the dressed potential, while free-free transitions become possible in the next order of the iteration. The study of the elastic scattering has already exhibited some interesting features [43]. The validity of the theory is, however, limited to cases where not only the earlier discussed condition of high frequency must be fulfilled, but also the incident energy of the electron is required to be small with respect to the photon energy. Under these circumstances, Feshbach resonances in the elastic or inelastic cross sections cannot occur. Here we will be interested in the case where, on one hand, the photon energy is large with respect to the ionization potential of the atom in the field, but, on the other hand, the energy of the incident electron is comparable or larger than the photon energy. It then becomes possible that the incident energy matches the ac Stark shifted levels of the atom in the field (modulo an integer number of the photon energy). Under these circumstances, the dynamics may lead to the emission of photons and cause the electron to be captured temporarily in a bound state of the dressed potential until the subsequent absorption of photons permits the electron to escape into the continuum again. The delay introduced by this capture-escape episode shows up as a resonance in the elastic and inelastic cross sections. Indeed, since there are two quantum paths involved in this scattering process (a "resonant" and a "nonresonant" path) leading to the same final state, as usual, interference will take place. This interference phenomenon will typically show up in the cross sections as a Fano-type profile on a smooth background, with a width that corresponds to the strong-field width of the hydrogen atom in the bound state at resonance. (As an illustration, see Ref. [44] for the result of a theoretical calculation of this effect in the case of weak fields.) Finally we note that these resonances are tunable either by varying the laser frequency at fixed energy of the incident beam of electrons or vice versa.

Let us finally discuss another way in which one may create the atom in the field in the deformed ground state. To this end the atom must be prepared in a certain $l$ mixture of states belonging to the same (high) principal quantum number, but having a magnetic quantum number $m = 0$. This initial state must be prepared in such a way that it resembles the dressed ground state (i.e., has a large overlap integral with it). By making the rise of the pulse short enough (square pulse), the wave function of the state under consideration will hardly undergo a significant change during this rise (*nonadiabatic* or *sudden* entrance of the pulse). On the other hand, during the entrance of the pulse, the wave function will start to oscillate like a free electron driven by the field. It may be possible that this situation can be realized before the atom has a chance to become ionized. The recorded multiphoton ionization signal will then be a fingerprint of the dynamics as predicted by our high-frequency theory. These dynamics will mark their signatures on the angular distributions of photoelectrons and the peak pattern in their energy spectrum as discussed in this paper and in a previous work [48].

## ACKNOWLEDGMENTS

The work presented here was carried out at the FOM—Institute for Atomic and Molecular Physics, Kruislaan 407, 1098 SJ Amsterdam, The Netherlands. It was part of the research program of the Stichting voor Fundamenteel Onderzoek der Materie (Foundation for the Fundamental Research on Matter) and was made possible by financial support from the Nederlandse Organisatie voor Wetenschappelijk Onderzoek (Netherlands Organization for the Advancement of Research). The author is greatly indebted to Dr. M. Gavrila, with whom he had many interesting and stimulating discussions. This work was finalized for publication by support of the National Science Foundation, under Grant No. PHY-9017079.

## APPENDIX A: THE MECHANISM UNDERLYING THE ANGULAR PATTERN OF PHOTOELECTRONS

In this appendix we will discuss the physical picture underlying the angular pattern of photoelectrons given by Eq. (10). This we will do by demonstrating that the multiphoton ionization amplitude corresponding to Eq. (10), given by Eqs. (12) and (13), can be thought of as generated by a certain *effective* density of sources $\rho_{\rm eff}(\mathbf{r},t)$. Here we will derive this effective density of sources in a heuristic way.

In what follows we will need the Fourier transform of the "end-point potential" $\tilde{V}_0(\mathbf{r})$ given by

$$\tilde{V}_0(\mathbf{r}) = -\frac{1}{\pi}\left(\frac{2}{\alpha_0 r}\right)^{1/2} K\left[\left(\frac{1-\cos\theta}{2}\right)^{1/2}\right], \tag{A1}$$

in terms of a complete elliptic integral of the first kind (see Ref. [2]). Similar to the case of the dressed potential $V_0$, the end-point potential can be looked upon as the electrostatic potential created by a (linear) charge distribution. By making use of the integral representation [45]

$$K\left[\left(\frac{1-\cos\theta}{2}\right)^{1/2}\right] = \tfrac{1}{2}\int_0^\infty \frac{du}{\sqrt{u}\sqrt{1+u^2+2u\cos\theta}}, \tag{A2}$$

Eq. (A1) can be cast in the form

$$\tilde{V}_0(\mathbf{r}) = -\frac{1}{\pi\sqrt{2\alpha_0}}\int_0^\infty \frac{du}{\sqrt{u}|\mathbf{r}+\mathbf{e}u|}. \tag{A3}$$

The Fourier transform of $\tilde{V}_0(\mathbf{r})$,

$$\tilde{\mathcal{V}}_0(\mathbf{k}) = \int d\mathbf{r} e^{-i\mathbf{k}\cdot\mathbf{r}}\tilde{V}_0(\mathbf{r}), \tag{A4}$$

can be easily evaluated using the integral form of Eq. (A3). By carrying out the integration with respect

to $\mathbf{r}$ first and by putting $u = \tau/|\mathbf{e}\cdot\mathbf{k}|$, we obtain

$$\tilde{V}_0(\mathbf{k}) = -\frac{2}{k^2}\left(\frac{2}{|\boldsymbol{\alpha}_0\cdot\mathbf{k}|}\right)^{1/2} \times \int_0^\infty \exp[i\,\mathrm{sgn}(\boldsymbol{\alpha}_0\cdot\mathbf{k})\tau]\tau^{-1/2}d\tau = -\frac{2\pi}{k^2}\left(\frac{2}{\pi|\boldsymbol{\alpha}_0\cdot\mathbf{k}|}\right)^{1/2}\exp\left(i\frac{\pi}{4}\mathrm{sgn}(\boldsymbol{\alpha}_0\cdot\mathbf{k})\right), \tag{A5}$$

where the integration with respect to $\tau$ was carried out in the complex plane along the positive or negative imaginary axis for $\boldsymbol{\alpha}_0\cdot\mathbf{k}$ positive or negative, respectively.

In order to discuss the mechanism of the multiphoton ionization process, we return to a dynamical, i.e., time-dependent picture. We will describe the process in the reference frame in which the proton oscillates according to $\mathbf{r} = -\boldsymbol{\alpha}(t)$ and in which external forces are absent (the Kramers frame). For sufficiently high frequencies, as was noted in Sec. V of paper I, the wave function of the *open-channel part* of the decaying state can be replaced to an excellent approximation by Eq. (62):

$$\tilde{\Psi}(\mathbf{r},t) = \int d\mathbf{r}' \int dt' \mathcal{G}_0^{(+)}(\mathbf{r},\mathbf{r}',t-t')\rho(\mathbf{r}',t'), \tag{A6}$$

in which the source density $\rho(\mathbf{r},t)$ is given by Eq. (63):

$$\rho(\mathbf{r},t) = -\frac{\Phi(-\boldsymbol{\alpha}(t))\exp(-iWt)}{|\mathbf{r}+\boldsymbol{\alpha}(t)|}. \tag{A7}$$

As we have discussed in Sec. II A, in the highly nonperturbative radiation regime the de Broglie wavelengths of the photoelectrons are small with respect to the spatial extension of the source from which they are emitted ($\alpha_0 k_n \gg 1$). The phase factor $\exp[i\boldsymbol{\alpha}(\phi)\cdot\mathbf{k}_n]$ associated with electron waves emitted at a position of the proton $-\boldsymbol{\alpha}(\phi)$ varies rapidly with the phase $\phi$ of the field. Consequently, waves emitted from different positions of the proton tend to cancel each other due to destructive interference. However, when the proton passes its turning points there is no such cancellation. This suggests that the angular dependence of photoelectrons arises from outgoing electron waves which are created near the turning points of the oscillation of the proton $\pm\boldsymbol{\alpha}_0$. Let us now construct an *effective* interaction potential exerted by the proton, which replaces $V(\mathbf{r}+\boldsymbol{\alpha}(t))$ $[= -1/|\mathbf{r}+\boldsymbol{\alpha}(t)|]$ in Eq. (A7). It can be shown from Eq. (11) of paper I that the Fourier time components of $V(\mathbf{r}+\boldsymbol{\alpha}(t))$, i.e., $V_n(\mathbf{r})$, have the following limiting behavior. For $\mathbf{r}\to+\boldsymbol{\alpha}_0$ we have

$$V_n(\mathbf{r}) \to (-1)^n \tilde{V}_0(\mathbf{r}-\boldsymbol{\alpha}_0), \tag{A8}$$

whereas for $\mathbf{r}\to-\boldsymbol{\alpha}_0$

$$V_n(\mathbf{r}) \to \tilde{V}_0(-\mathbf{r}-\boldsymbol{\alpha}_0). \tag{A9}$$

As is displayed, the limiting potential $\tilde{V}_0$ is the same for all Fourier components. In the case $n=0$, we already encountered it when studying the mechanism underlying the splitting of the (bound) electron cloud in fields of high $\alpha_0$ (the dichotomy; see Ref. [2]). Using Eq. (10) of paper I to carry out the Fourier synthesis leads to

$$V(\mathbf{r}+\boldsymbol{\alpha}(t)) \simeq \tilde{V}_0(\mathbf{r}-\boldsymbol{\alpha}_0)T\sum_{n=-\infty}^{+\infty}\delta(t-(n+\tfrac{1}{2})T) \tag{A10}$$

if $\mathbf{r}\simeq+\boldsymbol{\alpha}_0$ and

$$V(\mathbf{r}+\boldsymbol{\alpha}(t)) \simeq \tilde{V}_0(-\mathbf{r}-\boldsymbol{\alpha}_0)T\sum_{n=-\infty}^{+\infty}\delta(t-nT) \tag{A11}$$

if $\mathbf{r}\simeq-\boldsymbol{\alpha}_0$. The addition of the contributions from each turning point, followed by the insertion in Eq. (A7), yields the following expression for the effective source density:

$$\rho_{\mathrm{eff}}(\mathbf{r},t) = \left(\Phi(+\boldsymbol{\alpha}_0)\tilde{V}_0(\mathbf{r}-\boldsymbol{\alpha}_0)T\sum_{n=-\infty}^{+\infty}\delta(t-(n+\tfrac{1}{2})T) + \Phi(-\boldsymbol{\alpha}_0)\tilde{V}_0(-\mathbf{r}-\boldsymbol{\alpha}_0)T\sum_{n=-\infty}^{+\infty}\delta(t-nT)\right) \times\exp(-iWt). \tag{A12}$$

It has the form of a train of $\delta$ pulses in time, multiplied either by $\tilde{V}_0(\mathbf{r}-\boldsymbol{\alpha}_0)\Phi(+\boldsymbol{\alpha}_0)\exp(-iWt)$ at times when the proton is in its extreme right-hand position, or with $\tilde{V}_0(-\mathbf{r}-\boldsymbol{\alpha}_0)\Phi(-\boldsymbol{\alpha}_0)\exp(-iWt)$ when the proton is in its extreme left-hand position. Thus the effective source of Eq. (A12) emits electron waves at the instants when the proton passes its turning points. By the insertion of Eq. (A12) into Eq. (A6), it can be shown [by carrying out the Floquet analysis of Eq. (A6) and by determining the asymptotic behavior of its Floquet components for large $|\mathbf{r}|$, following Eq. (6) of paper I] that Eq. (A12) yields a multiphoton ionization amplitude of the form of Eq. (12), i.e.,

$$f_n = f_- + (-1)^n f_+. \tag{A13}$$

The amplitudes $f_\pm$ appearing in this equation are given by

$$f_\pm = -\frac{1}{2\pi}\exp(\mp i\boldsymbol{\alpha}_0\cdot\mathbf{k})\Phi(\pm\boldsymbol{\alpha}_0)|\tilde{V}_0(\mathbf{k})| \times\exp[\pm i\arg\tilde{V}_0(\mathbf{k})], \tag{A14}$$

in which $\tilde{V}_0(\mathbf{k})$ is defined by the Fourier transform of the end-point potential. When substituting Eq. (A5) into Eq. (A14) we see that our heuristically derived expression for the multiphoton ionization amplitude coincides with Eqs. (12) and (13).

Thus we have shown that the angular distribution of photoelectrons Eq. (10) can be thought of as created by the density of sources given in Eq. (A12). This justifies the dynamical picture which we have given to the rate at which photoelectrons are ejected as a function of the angle, Eq. (10).

## APPENDIX B: DERIVATION OF EQ. (20)

In this appendix we evaluate the integral

$$I_{m,n}(x) = \int_0^x J_m(\tau)J_n(\tau)d\tau, \tag{B1}$$

with $m+n$ even, for large values of its argument. For this purpose we introduce the auxiliary function

$$\tilde{I}_{m,n}(x;\lambda) = \int_x^\infty J_m(\tau)J_n(\tau)\tau^{-\lambda}d\tau, \tag{B2}$$

where $0 < \lambda < 1$. Thus we may express $I_{m,n}(x)$ in terms of $\tilde{I}_{m,n}(x;\lambda)$ as

$$I_{m,n}(x) = \lim_{\lambda \downarrow 0}[\tilde{I}_{m,n}(0;\lambda) - \tilde{I}_{m,n}(x;\lambda)]. \tag{B3}$$

For the moment we restrict $m$ and $n$ to non-negative values. Let us consider first the integral $\tilde{I}_{m,n}(x;\lambda)$ if $x$ is identically zero. It has the value [46]

$$\tilde{I}_{m,n}(0;\lambda) = \frac{\Gamma(\lambda)\Gamma((m+n-\lambda+1)/2)}{2^\lambda\Gamma((m-n+\lambda+1)/2)\Gamma((m+n+\lambda+1)/2)\Gamma((n-m+\lambda+1)/2)}. \tag{B4}$$

This expression can be readily expanded in a Laurent series about $\lambda = 0$, yielding

$$\tilde{I}_{m,n}(0;\lambda) = \frac{(-1)^{(m-n)/2}}{\pi\lambda} + \frac{(-1)^{(m-n)/2)}}{\pi}\left[\psi(1) - \ln 2 - \psi\left(\frac{m+n+1}{2}\right) - \psi\left(\frac{m-n+1}{2}\right)\right] + O(\lambda). \tag{B5}$$

Consider now the integral $\tilde{I}_{m,n}(x;\lambda)$ if $x$ is large. By replacing in Eq. (B2) the Bessel functions by their asymptotic series for large arguments [17], we obtain

$$\begin{aligned}\tilde{I}_{m,n}(x;\lambda) &= \frac{2}{\pi}\int_x^\infty \tau^{-\lambda-1}\cos\left(\tau - \frac{1}{2}m\pi - \frac{\pi}{4}\right)\cos\left(\tau - \frac{1}{2}n\pi - \frac{\pi}{4}\right)d\tau + O(x^{-\lambda-2}) \\ &= \frac{(-1)^{(m-n)/2}}{\pi}\int_x^\infty \tau^{-\lambda-1}d\tau + \frac{(-1)^{(m+n)/2}}{\pi}\int_x^\infty \tau^{-\lambda-1}\sin 2\tau\, d\tau + O(x^{-\lambda-2}) \\ &= \frac{(-1)^{(m-n)/2}}{\pi\lambda}x^{-\lambda} + O(x^{-\lambda-1}).\end{aligned} \tag{B6}$$

By the substitution of the results of Eqs. (B5) and (B6) in Eq. (B3) we obtain

$$I_{m,n}(x) = \frac{(-1)^{(m-n)/2}}{\pi}\left[\ln(2x) - \psi\left(\frac{m+n+1}{2}\right) - \psi\left(\frac{m-n+1}{2}\right) + \psi\left(\frac{1}{2}\right)\right] + O(x^{-1}), \tag{B7}$$

where we have made use of the relation $\psi(1) - 2\ln 2 = \psi(\frac{1}{2})$. The final relation holds irrespective of the signs of $m$ and $n$. This one may be easily verified from the relations $J_{-n}(x) = (-1)^n J_n(x)$ in Eq. (B1) and $\psi(-n+\frac{1}{2}) = \psi(n+\frac{1}{2})$ in Eq. (B7).

## APPENDIX C: DERIVATION OF EQ. (25)

In this appendix it will be shown that the sum $S_n^{(2)}$ of Eq. (23),

$$S_n^{(2)} = {\sum_{p,q}}' \Phi_{n-p}\Phi_{n-q}^*\left[2\psi\left(\frac{1}{2}\right) - \psi\left(\frac{p+q+1}{2}\right) - \psi\left(\frac{p-q+1}{2}\right)\right], \tag{C1}$$

can be cast in the integral form of Eq. (25):

$$S_n^{(2)} = 2\int_0^{\pi/2} \frac{|\Phi(\alpha_0\cos\phi)|^2\cos^2 n\phi - |\Phi(\alpha_0)|^2}{\sin\phi}d\phi. \tag{C2}$$

To do this we make use of the following integral representation of the $\psi$ function for half-integer values of its argument [47]:

$$\psi(m+\tfrac{1}{2}) - \psi(\tfrac{1}{2}) = \int_0^{\pi/2}\frac{1-\cos 2m\phi}{\sin\phi}d\phi. \tag{C3}$$

From this we have

$$2\psi(\tfrac{1}{2}) - \psi\left(\frac{p+q+1}{2}\right) - \psi\left(\frac{p-q+1}{2}\right) = 2\int_0^{\pi/2} \frac{\cos p\phi \cos q\phi - 1}{\sin\phi} d\phi. \tag{C4}$$

Consequently

$$S_n^{(2)} = 2\int_0^{\pi/2} \frac{C_n(\phi) - C_n(0)}{\sin\phi} d\phi, \tag{C5}$$

where we have denoted $C_n(\phi)$ by

$$C_n(\phi) = \sum_{p,q}{}' \Phi_{n-p}\Phi^*_{n-q} \cos p\phi \cos q\phi. \tag{C6}$$

The summation can be carried out with the help of Eq. (3). This yields

$$C_n(\phi) = |\Phi(\alpha_0 \cos\phi)|^2 \cos^2 n\phi, \tag{C7}$$

where we have assumed that the bound initial state $\Phi$ has definite parity. We thus find from Eqs. (C5) and (C7) the result of Eq. (C2).


[1] M. Gavrila and J. Z. Kaminski, Phys. Rev. Lett. **52**, 614 (1984), and unpublished; M. Gavrila, in *Atoms in Unusual Situations*, Vol. 143 of *NATO Advanced Study Institute, Series B: Physics*, edited by J. P. Briand (Plenum, New York, 1987), p.225.

[2] For a detailed study of the radiative distortion of the hydrogen atom in a linearly polarized field, see M. Pont, N. Walet, M. Gavrila, and C. W. McCurdy, Phys. Rev. Lett. **61**, 939 (1988); M. Pont, N. Walet, and M. Gavrila, Phys. Rev. A **41**, 477 (1990).

[3] M. Pont, M.J. Offerhaus, and M. Gavrila, Z. Phys. **9**, 297 (1988); M. Pont, Phys. Rev. A **40**, 5659 (1989).

[4] M. Pont, preceding paper, Phys. Rev. A **44**, 2141 (1991).

[5] We would like to recall here that Eq. (1) was derived from Eq. (15) of Ref. [4], obtained to lowest order in the inverse frequency. It should be valid irrespective of the value of $\alpha_0$, if the condition $\omega \gg |E_0(\alpha_0)|$ is well enough satisfied. The validity of Eq. (15) of Ref. [4] was assessed by estimation of the next term in the iteration in inverse powers of the frequency, a point which is supported by exact numerical calculations (see Ref. [27]). As such, some caution has to be taken with respect to mathematical rigor. As frequently happens with iterative procedures applied in theoretical physics, our high-frequency iteration scheme too is expected to be of the asymptotic type, i.e., formally divergent. What one would like to have is a rigorous bound on the error introduced when truncating the (asymptotic) series, but the most one may hope to be able to achieve is to prove that the truncation error is of some order in $\omega/|E_0(\alpha_0)|$. It should be realized that even with such a statement in hand, all *practical* calculations based on the Gavrila-Kaminski theory, derived from either Eq. (15) of Ref. [4] or (1) of the present paper, will still be subject to uncertainty. Although we realize the importance of such rigorous mathematical statements, it would carry us too far into mathematical physics, away from our main goal. With this in mind, we have chosen a more practical point of view.

[6] M. Bashkansky, P.H. Bucksbaum, and D.W. Shuhmacher, Phys. Rev. Lett. **60**, 2458 (1988).

[7] The consequences of our simplified expression for the total multiphoton ionization rate in superintense laser fields have very recently been examined for the case of atomic hydrogen and *circular* polarization by M. Pont and M. Gavrila, Phys. Rev. Lett. **65**, 2362 (1990).

[8] L. V. Keldysh, Zh. Eksp. Teor. Fiz. **47**, 1945 (1964) [Sov. Phys.—JETP **20**, 1307 (1965)].

[9] M. H. Mittleman, Phys. Lett. **47A**, 55 (1974).

[10] G. J. Pert, J. Phys. B **8**, L173 (1975).

[11] H. R. Reiss, Phys. Rev. A **22**, 1786 (1980).

[12] D. M. Volkov, Z. Phys. **94**, 250 (1935).

[13] M. H. Mittleman, *Theory of Laser-Atom Interactions* (Plenum, New York, 1982).

[14] M. Janjusevic and M. H. Mittleman, J. Phys. B **21**, 2279 (1988).

[15] The inclusion of the distortion of the initial state requires special care. It is incorrect to first neglect the electron-nucleus attraction and then to bring in the electrostatic interaction as a corrective term. Such a procedure is applicable only for channels that are open for decay (corresponding to unbounded motion of the electron), but not for the closed ones (corresponding to bounded motion). These latter ones are, however, essential for the description of the distorted initial state. This was later realized by Mittleman (private communication). It is therefore not surprising that the results of Janjusevic and Mittleman are in sharp conflict with mine, presented in this paper; see, however, Refs. [18,19] of paper I.

[16] I. S. Gradsteyn and I. M. Ryzhik, *Table of Integrals, Series and Products* (Academic, New York, 1980), formula 8.402.

[17] I. S. Gradsteyn and I. M. Ryzhik, *Table of Integrals, Series and Products* (Ref. [16]), formula 8.451.

[18] G. Leuchs and H. Walther, in *Multiphoton Ionization of Atoms*, edited by S. L. Chin and P. Lambropoulos (Academic, New York, 1984), Chap. 5.

[19] H. J. Humpert, H. Schwier, R. Hippler, and H. O. Lutz, Phys. Rev. A **32**, 3787 (1985).

[20] B. Wolff, H. Rottke, D. Feldmann, and K. Welge, Z. Phys. D **10**, 35 (1988).

[21] Note that whereas the wiggle energy of a free electron is a purely classical quantity (it does not depend on Planck's constant), the photon energy obviously is not. In the limit that Planck's constant goes to zero (the classical limit), Eq. (17) is automatically satisfied. One might therefore think that in the highly nonperturbative radiation regime our theory becomes classical. This conclusion is, however, incorrect, for in order for the Gavrila-Kaminski theory to be applicable, the high-frequency condition must be fulfilled. As is easily shown, this latter condition excludes the classical domain.

[22] P. Kruit, J. Kimman, H. G. Muller, and M. J. van der Wiel, Phys. Rev. A **28**, 248 (1983).

[23] P. H. Bucksbaum, M. Bashkansky, R. R. Freeman, T. J. McIlrath, and L. F. DiMauro, Phys. Rev. Lett. **56**, 2590 (1986).

[24] R. M. Potvliege and R. Shakeshaft, Phys. Rev. A **38**, 6190 (1988); M. Dörr and R.M. Potvliege, *ibid.* **41**, 1472 (1989). The relevance of shadow states in the passage from low to high intensities at fixed low frequency is discussed in M. Dörr, R. M. Potvliege, D. Proulx, and R. Shakeshaft (unpublished). This work is particularly interesting, since a comparison of our high-frequency data with accurate Floquet calculations was made for atomic hydrogen. The applicability of their method is, however, restricted to relatively low values of $\alpha_0$ (private communication).

[25] Compare in this context Eq. (40) with the corresponding expression for circular polarization, Eq. (12) of M. Pont and M. Gavrila, Phys. Rev. Lett. **65**, 2362 (1990).

[26] The energy eigenvalues for the cases $\alpha_0 = 400$ and 1000 for the ground state of atomic hydrogen were not given in Ref. [2]; these values amount to $-0.010\,31$ and $-0.005\,588$, respectively.

[27] The convergence of the Gavrila-Kaminski theory was tested on one-dimensional model atoms with short-range potentials, both for multiphoton ionization and scattering. The case of *ionization* was considered by J. N. Bardsley and M. J. Comella, Phys. Rev. A **39**, 2252 (1989). The Floquet system of equations was solved numerically and compared to the single Floquet-channel calculation based on Eq. (15) of Ref. [4]. The results obtained for the (real part of the) high-frequency eigenvalues agree remarkably well with those predicted by Eq. (15) of the preceding paper, even at the relatively low photon energies $2.5 < \omega/|E_0(\alpha_0)| < 5$, where $|E_0(\alpha_0)|$ is the binding energy of the ground state. R. Bhatt, B. Piraux, and K. Burnett, Phys. Rev. A **37**, 98 (1988), considered the case of *scattering* (free-free transitions). Again, by solving numerically the Floquet system in the Kramers frame of reference, they obtained results for the multiphoton transition amplitudes and compared their magnitudes to the elastic amplitudes [corresponding to Eq. (15) of Ref. [4]]. The results indicate the decrease at high frequencies of the former with respect to the latter one [see their Fig. (5a)], as required by our high-frequency theory.

[28] *Ultrafast Phenomena VI*, edited by T. Yajima, K. Yoshihara, C. B. Harris, and S. Shionoya (Springer-Verlag, Berlin, 1988).

[29] By an ideal experiment we mean an experiment that satisfies the assumptions of our theory.

[30] From Eq. (33) we have for $\alpha_0$ sufficiently high $|u(\mathbf{0})|^2 \simeq 2\alpha_0|\Phi(\alpha_0)|^2$. For $\alpha_0 = 1000$ we find $|\Phi(\alpha_0)| = 0.002\,61$ and we thus obtain $|u(\mathbf{0})|^2 = 0.0136$. The numerical values of the constants $C_1$ and $C_2$ of Eq. (36) can be calculated from Eqs. (30) and (31). This yields, for $\alpha_0$ sufficiently large,

$$C_1 \simeq \int_0^{\alpha_0^{1/3}} \frac{|\Phi(\alpha_0 - \mathrm{e}x)|^2 - |\Phi(\alpha_0)|^2}{|\Phi(\alpha_0)|^2 x}\,dx$$

and

$$C_2 \simeq \int_{\alpha_0^{1/3}}^{\alpha_0} \frac{|\Phi(\alpha_0 - \mathrm{e}x)|^2}{|\Phi(\alpha_0)|^2 x}\,dx.$$

By evaluating the indicated integrals for $\alpha_0 = 1000$, we obtain $C_1 = 1.07$ and $C_2 = 2.71$.

[31] N. R. Walet, Phys. Rev. A **41**, 3905 (1990). For higher $\omega$ the agreement is not as good. This is likely to be ascribed to the fact that at high frequencies the final-state wave function oscillates rapidly in space. In the latter case a rather small mesh size is needed in order to obtain good convergence and this could not be handled in the reference given above. This problem was realized by this author, however, and is also apparent from his "$\omega = \infty$" point, which should yield zero, but yields instead a nonzero value because of the limited accuracy of his computation (see his Fig. 9).

[32] R. M. Potvliege and R. Shakeshaft, Phys. Rev. A **40**, 3061 (1989).

[33] C. K. Rhodes (unpublished).

[34] D. L. Matthews and M. D. Rosen, Sci. Am. **12**, 60 (1988).

[35] P. Lambropoulos, Phys. Rev. Lett. **55**, 2141 (1985).

[36] Due to the large centrifugal barrier associated with the rotation of the electron about the polarization axis if $m$ is high, the probability of finding the electron near the polarization axis is very small. As we have seen in Sec. V of the preceding paper, ionization in high-frequency fields is initiated very close to the nucleus. Although we have worked out the case of $\sigma$ states only, our physical arguments in Sec. V of the preceding paper do apply to non-$\sigma$ states as well. [This can be shown from formulas similar to Eq. (67) of Ref. [4], valid for non-$\sigma$ states.] Combining these two notions leads to our above-stated conjecture.

[37] A. ten Wolde, L. D. Noordam, A. Lagendijk, and H. B. van Linden van den Heuvell, Phys. Rev. Lett. **61**, 2099 (1988).

[38] F. H. M. Faisal, *Theory of Multiphoton Processes* (Plenum, New York, 1985), Chap. 12.

[39] M. Gavrila, in *Collision Theory of Atoms and Molecules*, Vol. 196 of *NATO Advanced Study Institute, Series B: Physics*, edited by F.A. Gianturco (Plenum, New York, 1989), p. 139.

[40] A. Weingartshofer, J. K. Holmes, J. Sabagh, and S. L. Chin, J. Phys. B **16**, 1805 (1983).

[41] L. Langhans, J. Phys. B **11**, 2361 (1978).

[42] M. Gavrila and J. Z. Kaminski, Phys. Rev. Lett. **52**, 614 (1984).

[43] J. van de Ree, J. Z. Kaminski, and M. Gavrila, Phys. Rev. A **37**, 4536 (1988).

[44] L. Dimou and F. H. M. Faisal, Phys. Rev. Lett. **59**, 872 (1987).

[45] P. F. Byrd and M. D. Friedman, *Handbook of Elliptic Integrals for Engineers and Scientists* (Springer, Berlin, 1971), formula 241.00.

[46] I. S. Gradsteyn and I. M. Ryzhik, *Table of Integrals, Se-*

*ries and Products* (Ref. [16]), formula 6.574.

[47] The relation $\psi(m+\frac{1}{2}) = \psi(-m+\frac{1}{2})$ confirms that the expression (C3) is indeed symmetric in $m$, so that it suffices to establish the proof of Eq. (C3) for $m \geq 0$. This readily follows by induction, making use of the well-known recurrence formula $\psi(z+1) = \psi(z) + 1/z$.

[48] M. Pont, Ph.D. thesis, University of Amsterdam, 1990 (unpublished).